To my family…

FUNCTIONALIZED BIOFILM PROTEINS FOR ANTIBIOTIC DEGRADATION AND SARS-CoV-2 CAPTURE

A THESIS SUBMITTED TO

THE GRADUATE SCHOOL OF ENGINEERING AND SCIENCE

OF BILKENT UNIVERSITY

IN PARTIAL FULFILLMENT OF THE REQUIREMENTS FOR

THE DEGREE OF

MASTER OF SCIENCE

IN

MATERIALS SCIENCE AND NANOTECHNOLOGY

By

GÖKÇE ÖZKUL

SEPTEMBER 2021

FUNCTIONALIZED BIOFILM PROTEINS FOR ANTIBIOTIC DEGRADATION AND SARS-CoV-2 CAPTURE

By Gökçe Özkul

September 2021

We certify that we have read this dissertation and that in our opinion it is fully adequate, in scope and in quality, as a thesis for the degree of Master of Science.

Urartu Özgür Şafak Şeker (Advisor)

Onur Çizmecioğlu

Cengizhan Öztürk

Approved for the Graduate School of Engineering and Science:

Ezhan Karaşan

Director of the Graduate School

ABSTRACT

FUNCTIONALIZED BIOFILM PROTEINS FOR ANTIBIOTIC DEGRADATION AND SARS-CoV-2 CAPTURE

Gökçe ÖZKUL

MSc in Materials Science and Nanotechnology

Advisor: Urartu Özgür Şafak ŞEKER

September, 2021

Among biomaterials, biofilm proteins occupy a great portion. They have many prominent properties such as mechanical strength, ability to be modified genetically and their stability against harsh physical and chemical conditions from their environment. Their high tendency to genetic modifications provides them wide application areas ranging from environmental pollution prevention to medical usage areas. Therefore, it is of crucial importance that biofilm proteins can handle different genetic modifications for a desired purpose of use.

In this thesis, we aimed to form complex structures of CsgA biofilm protein with three different functional groups. The functional groups we used are laccase type enzymes, i.e. CotA and YlmD, and a lectin, Griffithsin (GRFT). The complex formation between CsgA biofilm protein and the aforementioned functional groups is achieved with the help of an irreversible bond formed when SpyTag-SpyCatcher

protein domains interact with each other. With the complexes we obtained from CsgA and CotA, YlmD enzymes we performed degradation of a fluoroquinolone type antibiotic, which is abundantly found in the natural water bodies causing antibiotic resistance. The degradation products of the antibiotic were assessed via LCMS-QTOF. We have also formed a complex from CsgA and GRFT in which we aimed to capture SARS-CoV-2 virus particles from aqueous media. We have checked the infectivity of SARS-CoV-2 virus after incubation with the complex we created.

In conclusion, CsgA biofilm protein can effectively be modified with various functional groups by making use of an irreversible chemical bond formed when a set of other proteins interact. The complex formed at the end can be used for different purposes such as pollutant degradation and virus capture. The complex system is prone to modifications with other functional groups for desired application areas.

Keywords: biofilm protein, functionalization, antibiotic degradation, virus capture, complex formation

ÖZET

FONKSİYONEL BİYOFİLM PROTEİNLERİNİN ANTİBİYOTİK GİDERİMİ VE SARS-COV-2 YAKALANMASI İÇİN KULLANIMI

Gökçe ÖZKUL

Malzeme Bilim ve Nanoteknoloji, Yüksek Lisans

Tez danışmanı: Urartu Özgür Şafak ŞEKER

Eylül, 2021

Biyomalzemeler arasında biyofilm proteinleri büyük bir yer kaplar. Mekanik dayanım, genetik olarak modifiye edilebilme ve çevrelerinden gelen zorlu fiziksel ve kimyasal koşullara karşı dayanıklılık gibi birçok öne çıkan özelliklere sahiptirler. Genetik modifikasyonlara olan eğilimlerinin yüksek olması, onlara çevre kirliliğinin önlenmesinden tıbbi kullanım alanlarına kadar geniş bir uygulama alanı sunmaktadır. Bu nedenle biyofilm proteinlerinin istenilen kullanım amacı için farklı genetik modifikasyonları işleyebilmesi çok önemlidir.

Bu tezde, CsgA biyofilm proteinden kompleks yapıları üç farklı fonksiyonel grupla oluşturmayı amaçladık. Kullanılan fonksiyonel gruplar, lakkaz tipi enzimler, yani CotA ve YlmD ve bir lektin olan Griffithsin (GRFT)'dir. CsgA biyofilm proteini ile yukarıda belirtilen fonksiyonel gruplar arasındaki kompleks oluşumu, SpyTag-SpyCatcher proteinlerinin birbirleriyle etkileşime girmesiyle oluşan kuvvetli bir bağ

yardımıyla sağlanır. CsgA biyofilm proteini ve CotA, YlmD enzimlerinden elde ettiğimiz kompleksler ile doğal su kütlelerinde bolca bulunan ve antibiyotik direncine neden olan florokinolon tipi bir antibiyotiğin parçalanmasını gerçekleştirdik. Antibiyotiğin parçalanması sonucu oluşan ürünler, LCMS-QTOF ile analiz edildi. Ayrıca sıvı ortamlarda bulunabilecek SARS-CoV-2 virüs partiküllerini yakalamayı amaçlayarak CsgA ve GRFT'den oluşan bir kompleks sistem gerçekleştirdik. Oluşturduğumuz kompleksle inkübe edildikten sonra SARS-CoV-2 virüsünün bulaşıcılığını kontrol ettik.

Sonuç olarak, CsgA biyofilm proteininin, çeşitli fonksiyonel gruplarla aralarında kurulacak kuvvetli bir kimyasal bağ ile etkili bir şekilde modifiye edilebileceği gösterildi. Elde edilen nihai kompleksin, çevresel kirliliklerin giderimi ve virüs yakalama gibi farklı amaçlar için kullanılabilir olduğu belirlendi. Geliştirilen kompleks sistem, farklı uygulama alanları için diğer fonksiyonel gruplarla modifikasyonlara uyumlu olarak tasarlandı.

Anahtar kelimeler: biyofilm proteini, fonksiyonelleştirme, antibiyotik giderimi, virüs yakalama, kompleks oluşumu

ACKNOWLEDGEMENTS

First of all, I would like to express my gratitude to my advisor Dr. Urartu Özgür Şafak Şeker. As an environmental engineer knowing very little about genetic engineering, he accepted me as a group member 3 years ago. During the time I spent in Dr. Şeker's group, I had the chance to develop new perspectives about things I can contribute to my profession, which I have also decided to pursue in the future as a career. I would like to thank him for the chance he gave me, for his trust and for his valuable mentorship on this journey of mine.

I would also like to thank my jury members Dr. Cengizhan Öztürk and Dr. Onur Çizmecioğlu for their valuable comments, reviewing my study and for their valuable time.

From the first day as a new member to the lab, Çisil Köksaldı was always there for me and helped me so much about getting used to everything about the lab. We spent so much time together both in and out the lab. She became a sister to me now. The ice cream breaks that we gave together, our lunches together, her limitless efforts to show me everything she knew about the lab are the reasons why I cannot thank her more. It would be so much harder if she was not around.

Regarding the times I first started the lab, Dr. Ebru Şahin Kehribar and Recep Erdem Ahan helped me so much with the problems I faced about my work. Their support meant so much for me while conducting my experiments. I would like to thank them for their comments, patience and limitless helps. I would like to thank them also for the fun times we had outside the lab. I thank Eray Ulaş Bozkurt for his friendship and for our chats during coffee breaks. I enjoyed the times we spent together with Çisil Köksaldı, Elif Özçelik and Gizem Makas during this stressful period of writing

master's thesis. I would like to specially thank to Gizem Makas for her kindness, support and positive energy. I would like to thank all present and former Synthetic Biosystems Laboratory group members; Ahmet Hınçer, Anooshay Khan, Dr. Behide Saltepe, Büşra Merve Kırpat, Cemile Elif Özçelik, Çisil Köksaldı, Dr. Ebru Aras, Dr. Ebru Şahin Kehribar, Dr. Esra Yuca, Eray Ulaş Bozkurt, Gozeel Binte Shadid, Julian Ostaku, Merve Erden Tüçer, Merve Yavuz, Murat Alp Güngen, Nedim Hacıosmanoğlu, Nedim Kurt, Recep Erdem Ahan, Sıla Köse, and Suat Tüçer. It was a privilege to be a part of this group and to work in a cooperative, friendly environment.

I want to thank my friends from UNAM, that we have been together since we took classes; Melis Özkan, Abtin Saateh, Can Çamiçi, Doğu Özyiğit, Kerem Kurban, Bouthaina Aoudi, and Joudy Maskoun. I enjoyed every moment we shared. I would also like to thank Zafer Koşar for his friendship and for our chats during coffee breaks. I would also like to thank my best friends from my undergraduate years at METU, Bengisu Uğurlu, İlayda Çakar, Melike Pektaş, and Merve Gülveren. They supported me in every decision and they were there for me every time I needed. I am lucky to have them as my best friends.

Lastly, I want to express my greatest gratitude and deepest thanks to my family for their endless support and love. I want to thank my mother Reyhan, my father Aykut and my little sister Göksu for being there any time I needed them. They have always been supporters of my decisions, my guides in the dark and my home. I could not have done this far and succeeded without their love and support.

TABLE OF CONTENTS

List of Tables

List of Figures

CHAPTER 1

INTRODUCTION

1.1. CsgA, Major Biofilm Protein

Biofilms are included in both living engineered materials and also in self-assembled materials categories. Biofilm structures are composed of amyloid fibers, which are regulated by a group of proteins and have a specific structure of cross-β strands [1]. This mentioned structure of cross-β strands enables a network of hydrogen bonding throughout the amyloid fibers. The resulting effect of this network structure is outstanding material properties including high Young's modulus and tensile strength [2]. As a result of all the prominent properties of amyloid fibers, many bacteria including *Escherichia coli* and *Bacillus subtili*s build biofilms for the purpose of protecting themselves from harsh conditions of their corresponding environment. Among the amyloid fibers the best studied one is the bacterial biofilm amyloids by *E. coli*. The amyloid formation in *E. coli* is controlled by a group of genes, namely curli-specific genes (*csg*) which consists of two operons *csgBAC* and *csgDEFG* [3]. The group of genes regulated by the *csg* operons have specific functions in the *E. coli* biofilm formation. To begin with, CsgA is known for the formation of major curli subunit (Figure 1). CsgB, which is the minor curli subunit, is responsible for the anchoring of fibers on the cell and also it has a role as the nucleator for gathering the secreted CsgA curli subunits into curli fibers. CsgG is a pore-forming lipoprotein special for the transportation of curli sub units CsgA and CsgB to outer membrane. Moreover, CsgG functions in harmony with CsgE and CsgF which are known to act as periplasmic and extracellular accessory proteins. CsgE directly binds to CsgA with the purpose of preventing CsgA from premature aggregation in the cytoplasm,

which may be lethal to cell during the transportation through the periplasm. In addition, CsgF is speculated to be exposed to the surface and it has a critical role in CsgB mediated nucleation of CsgA fibers. Moreover, *csgBAC* operon has a transcriptional factor regulating it, CsgD, which supposedly has a control over the timely expression of both *csg* operons. Finally, CsgC has no known reported function in curli formation but it is a presumed oxidoreductase [3]. However, recently CsgC is reported to have a similar function as CsgE that it prevents early maturation of CsgA in the cytoplasm, protecting the cell from a potential lethal situation [4].

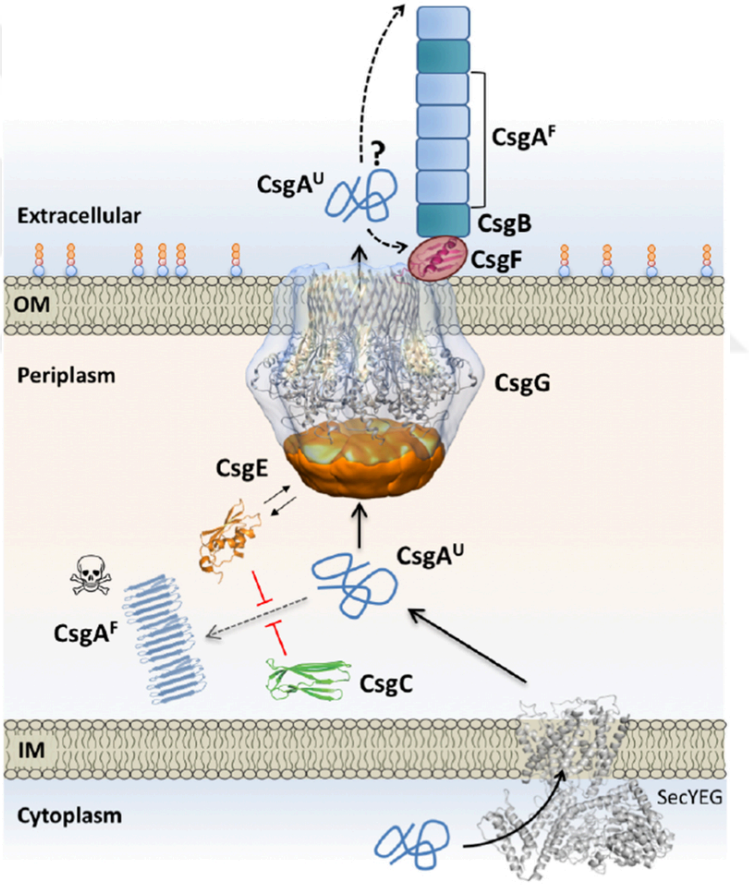

Figure 1. Schematic representation of CsgA production in the cell regulated by *csgBAC* and *csgDEFG* operons [4]. Reprinted from Bhoite, Gerven, Chapman, Remaut, 2019.

In addition to the secretion mechanism of *E. coli* curli fibers, major and minor curli proteins of the system have some specific architecture. N terminals of both CsgA and CsgB subunits include a signal sequence, which is cleaved upon transfer to the periplasmic space. The subunits also exert a curli-specific targeting sequence, which is followed by 5 pseudo-repeats. These repeating regions are known to form the basis of amyloid structure of the curli subunits [5].

1.2. CsgA as Engineered Biomaterial

Due to high tendency to genetic modifications, CsgA can be engineered practically for a wide range of application areas, such as biomaterials with prominent physical properties, or biomaterials for environmental protection against pollutants and even biomaterials for medical applications. Some recent research brought different uses of CsgA upon modifications into the light. There have been some very enlightening studies both from past and recent times. To start with a recent example, CsgA has been modified to develop an advanced bioink for 3D printers with improved physical properties. The genetic modification for obtaining more robust CsgA fibers rooted from the phenomena of blood clot formation. They fused knob-hole fibrin monomers to CsgA proteins leading to polymerization of fibrins via noncovalent interactions. This system eventually led to formation of the shear-thinning hydrogel of CsgA with desired viscoelastic performance suitable for use as bioink [6]. Moreover, CsgA has been used to create a water-processable and biodegradable material, which was tested to be suitable for welding and healing in the presence of water. In this study, CsgA was fused with human trefoil factor 2 (TFF2) which enabled them to harvest biofilm proteins in hydrogel form. This fusion protein of CsgA with TFF2 was then used to cast onto surfaces or mold into plastic films [7]. Another example of

functionalized CsgA application area was capturing Influenza viruses from aqueous media. By fusing a peptide known for its ability to bind Influenza virus to downstream of CsgA major curli subunit, a biofilm matrix that is able to capture virus particles was formed [8]. Lastly, CsgA was also functionalized by an enzyme known as alkaline phosphatase, ALP, in order to show enzymes are more stable when they are fused to CsgA biofilm protein due to its robust nature and also in order to show that enzymes can be catalytically active in when fused to CsgA. This resulted in the idea that enzyme fused CsgA biofilm proteins can be formed and used against environmental pollution prevention [9]. Rooting from these examples of different application areas of functionalized CsgA curli fibers, CsgA can be stated as an adjustable raw material for genetic engineering in order to incorporate various functionalities. As a result, there are a wide range of functional groups that can be fused with CsgA for incorporation of functional properties.

1.2.1. Enzyme Functionalized Biofilm Proteins

Biofilm protein CsgA can be functionalized with various other proteins and tags to have improved properties in different application areas. The modifications may enhance material properties of the biofilm protein and thus lead to be considered as promising raw materials in already existing industries [7,10]. In addition, CsgA fused protein domains may provide new functionalities such as catalytic activity that would eventually result in new application areas with further engineering such as bioremediation [9].

Enzymes are included in the formerly mentioned modifications that can be done on biofilm protein CsgA to have a catalytic activity. Laccases are enzymes known for

their catalytic activity against aromatic compounds such as phenols, and anilines via a mechanism of electron transfer to molecular oxygen [11]. Laccases regardless of being originated from fungus or bacteria, have 3 sequentially arranged cupredoxin like domains, which consist of β barrels made of β sheets and β strands and are able to bind copper [12]. Laccases have 4 copper atoms with 3 types, Type 1 copper (T1Cu), Type 2 copper (T2Cu), and Type 3 copper (T3Cu). These copper atoms are involved in the catalytic mechanism of laccases. The mechanism is believed to start with reduction of Type 1 copper by reducing substrate followed by transfer of internal electron from Type 1 copper to Type 2 and Type 3 copper and finally continue with the reduction of O_2 to H_2O at Type 2 and Type 3 copper sites [12–14].

Despite the fact that laccases are mainly produced by white-rot fungi and some plants, fungal laccases are not suitable for wide range applications in industry due to high fermentation periods, low enzyme yields, and low activity under working conditions such as high temperature, pH and salt concentrations [15,16]. However, recently bacterial laccases gain attention as a result of their prominent properties with respect to fungi originated laccases. Bacterial laccases have higher enzymatic activity under severe conditions such as highly varied temperatures and pH in addition to being robustly stable against inhibitory agents [17]. Moreover, they are beneficial when considering broad range of substrate specificity, shorter production time, ability to be cloned, expressed and manipulated in a host organism and being cost effective [18,19].

Laccases are known to oxidize phenolic and non-phenolic substrates [12]. The oxidation of phenolic substrates is driven by the difference of redox potentials

between T1 copper site of the enzyme and the corresponding substrate. In addition to phenolic substances, laccases are known to degrade non-phenolic substances in the presence of mediators. One of the most commonly used mediators is known to be 2,2'-azinobis-(3-ethylbenzthiazoline-6-sulfonate) (ABTS), which helps the oxidation reaction by providing an electron transfer mechanism [12].

Among these bacterial laccases, outer endospore coat protein of *Bacillus subtilis* strain 168, CotA encoded by *cotA*, is a monomeric protein and known to have laccase activity which has been characterized and studied earlier [14,20,21]. CotA is a copper dependent laccase known for its role in the biosynthesis of brown spore pigment, a melanin-like product, for *B. subtilis* which acts as a protective shield against the UV light and H_2O_2 for the spore [12]. Therefore, CotA can be used to functionalize major curli subunit CsgA and therefore has the ability to enzymatically degrade aromatic compounds when it is fused with CsgA with the help of cupredoxin domains found in its structure [14].

Furthermore, *B. subtilis* strain 168 also exerts a protein, YlmD (UniProtKB – O31726), which is referred as a laccase domain protein. It shows molecular functions such as copper ion binding, and oxidoreductase activity, which are characteristic properties of bacterial laccases according to UniProtKB [22]. Therefore, YlmD can also be used in order to functionalize CsgA biofilm fibers.

The mentioned laccases, CotA and YlmD, are known for degrading fluoroquinolone type antibiotic compounds such as Ciprofloxacin. Ciprofloxacin is a synthetic fluoroquinolone that is widely prescribed for human infections such as urinary tract infections [23]. It is also a widely used antibiotic in veterinary medicine. Due to

frequent use of Ciprofloxacin its presence in the nature cannot be ignored since it poses a threat to emergence of naturally found antibiotic resistant microorganisms [24]. At this point, the aforementioned laccase enzymes have a big role in the degradation of antibiotics such as Ciprofloxacin. The enzymes are known to preferably attack the piperazinyl ring that is found in the chemical structure of the antibiotic [24]. Moreover, the products after degradation of Ciprofloxacin with laccases are also identified by several studies via mass spectroscopy analysis [23–25]. As a result, considering the natural abundance of Ciprofloxacin and the ability of CotA and YlmD laccases to degrade Ciprofloxacin, the functionalization of CsgA with the mentioned enzymes could be a way to eliminate Ciprofloxacin from environment and eventually a way to prevent occurrence of naturally found antibiotic resistant microorganisms.

1.2.2. Griffithsin Fused Biofilm Proteins

Griffithsin (GRFT) is a red-algae (*Griffithsia sp.*) originated carbohydrate binding protein, i.e. lectin, which is known for its antiviral properties [26,27]. Antiviral property of GRFT stems from its high targeting affinity against mannose groups, which are observed as oligomannose glycoproteins on enveloped viruses [28]. Examples for these enveloped viruses that GRFT is found to be effective may be given as Human Immunodeficiency Virus (HIV-1), and Hepatitis C Virus (HCV) [29–31]. The antiviral property of GRFT roots to the ability of blocking viral internalization step due to high binding affinity against surface glycoproteins of viruses. For example, it has been previously shown that GRFT binds gp-120 surface protein of HIV-1 [32] and S protein of SARS-CoV [33] and MERS-CoV [34] through the mentioned mechanism. Moreover, for the pandemic that the earth has

been facing for the last 2 years that is caused due to new coronavirus, SARS-CoV-2, was also investigated against possible antiviral activity of GRFT. According to the results, it was proven that GRFT was effective against binding to the glycan structures of S protein of SARS-CoV-2 virus, which prevents the viral internalization by the cells leading to an antiviral effect at the end [35]. Therefore, functionalization of CsgA with GRFT lectin could serve for various applications. It could be used for capturing SARS-CoV-2 virus particles from the environment, and eventually could lead to decreased viral activity at the source of the virus.

1.2.3. SpyTag – SpyCatcher Fused Biofilm Proteins

Streptococcus pyogenes, a Gram-positive bacterium, is known for its extracellular proteins which are stabilized by spontaneous isopeptide bonds. The exploration of SpyTag peptide and its protein partner SpyCatcher was achieved through the analysis of immunoglobulin-like collagen adhesin domain, i.e. CnaB2, from fibronectin binding protein FbaB of *S. pyrogenes* species [36]. Knowing the fact that CnaB2 domain consists of a single isopeptide bond, which enables CnaB2 to have exceptional stability at very low pH and very high temperature [37], the protein domain was separated into a 13 amino acid peptide tag and 138 amino acid protein partner following modifications made in the mentioned parts. The peptide tag, which is named as SpyTag, can form strong intramolecular isopeptide bond with its protein partner named as SpyCatcher in a favorable reaction media [36]. According to crystallography and NMR, the bond formation happens between the unprotonated amine of Lys^{31} and carbonyl carbon of Asp^{117}, which occurs as a result of nucleophilic attack catalyzed by the neighboring Glu^{77} [36]. Therefore, the separation

of the peptide tag and protein partner was done so that the peptide contained reactive Asp and the protein partner contained the rest of the original protein [36].

The application areas of SpyTag and SpyCatcher system has widened in time. One example is the use of SpyTag peptide tag for protein purification such that, through consecutive engineering steps, Spy&Go system was generated, which allowed purification and elution of SpyTag fusion proteins with an admirable purity than that of His-tag [38]. In addition to many application areas such as attachment to surfaces or particles, diversifying protein function and enzyme assembly [39–42], SpyTag-SpyCatcher peptide-protein duo is also used for functionalizing *E coli* major curli protein CsgA. They have been previously used to provide catalytic properties to CsgA [43], to decorate major curli protein with gold nanoparticles or quantum dots [44], and to form a solid support for a cascade of multi-enzyme assembly [41]. Other than the stated examples, SpyTag-SpyCatcher dual system could also be used for combining different protein domains to each other via the irreversible isopeptide bond formed between SpyTag and SpyCatcher. Such as combining CsgA fibers with functional groups like enzymes or lectins by fusing the SpyTag and SpyCatcher domains separately to the desired proteins that are planned to be fused with each other.

1.3. Objective of the Study

In this study, we aimed to functionalize *E. coli* major curli biofilm protein CsgA such that it could be engineered for different purposes of use. We used two types of laccase enzymes, CotA and YlmD, originating from *B. subtilis* and a lectin, Griffithsin, known for its high binding affinity against multiple mannose groups found in envelope proteins of viruses. By making use of these three functional biofilm protein complexes, we first aim to degrade a widely found antibiotic in wastewaters, i.e. Ciprofloxacin, which otherwise cannot be very effectively degraded in conventional wastewater treatment plants and we aimed to identify the degradation products via LCMS-QTOF. Secondly, we focused on capturing SARS-CoV-2 virus particles from aqueous media such as wastewaters with the help of GRFT lectin by using its ability to bind glycans of surface proteins of enveloped viruses (Figure 2). As a result, we aim to form 3 different complexes of CsgA with enzymes and lectins via the bridging property of SpyTag and SpyCatcher domains with the help of irreversible isopeptide bond formed between them.

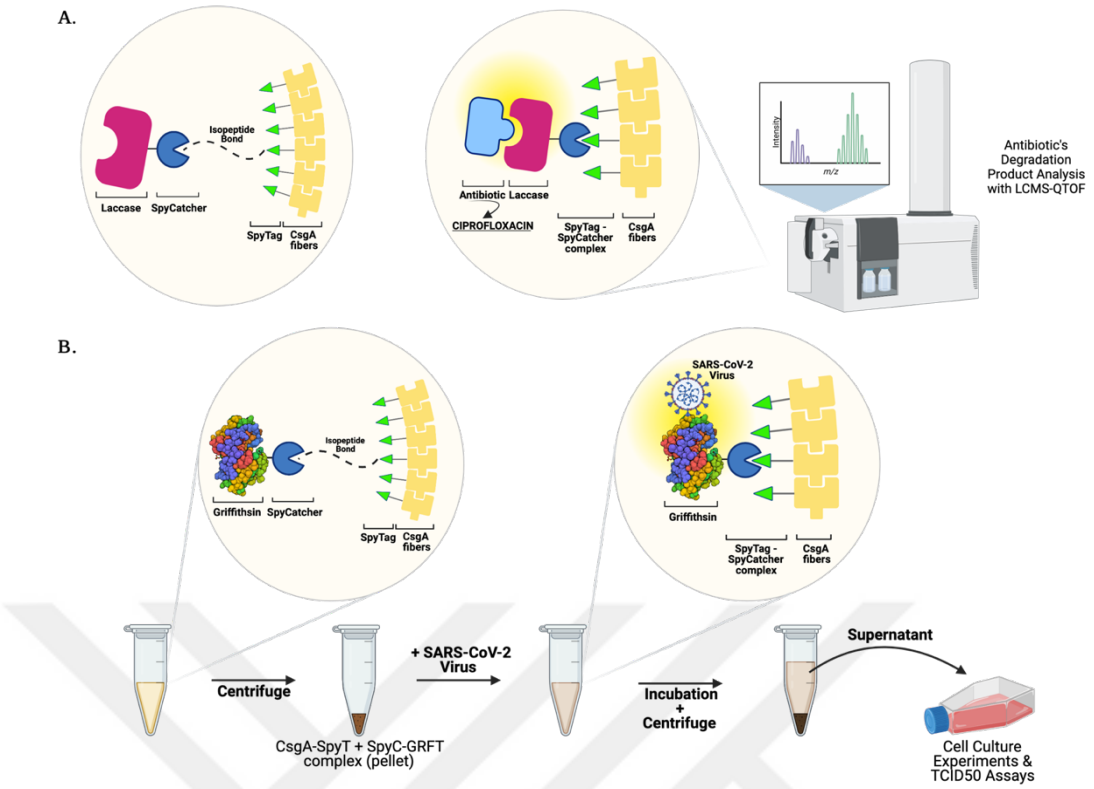

Figure 2. Schematic representation of functionalized CsgA fibers for A. antibiotic degradation and B. SARS-CoV-2 capture. Illustration is created using Biorender.com

CHAPTER 2

MATERIALS AND METHODS

2.1. Cell Strains, Growth, Transformation and Cell Maintenance

E. coli DH5α strain was used for cloning purposes. *E. coli* DH5α strain is suitable for cloning due to its high insert stability, high yield and quality of DNA regarding mutations in *recA1* and *endA* genes, respectively. For recombinant protein expression, *E coli* BL21 DE3 strain was used. This strain encodes T7 polymerase under the control of Lac promoter and is deficient of proteases for high yield recombinant protein expression. For biofilm experiments, *E. coli* K12 strain (ΔcsgA strain) which lacks *csgA* gene was used. All the cell strains were stored at -80ºC in Lysogeny Broth (LB) medium (recipe given in Appendix E, Table E.1) containing 25% glycerol.

Plasmids were transformed into mentioned bacterial cells via chemical transformation. Preparation of chemical competent cells for *E coli* DH5α, BL21 DE3 and ΔcsgA strains was achieved by inoculating cells from -80ºC cell stock and by growing both cells overnight in LB medium with proper antibiotics supplied. Following overnight inoculation, the cells were diluted 1:100 into fresh LB supplied with proper antibiotics and grown until OD_{600} reaches 0.2 – 0.5. Once this point was achieved, the cells were cooled on ice for 10 minutes. After, cells were collected by centrifugation at 1000xg for 10 minutes at 4ºC. Supernatant was removed and the cell pellet was resuspended in Transformation and Storage Buffer (TSS) (PEG 8000 20% (w/v), DMSO 10% (w/v), $MgCl_2$ 100mM, pH 6.5 in LB) with an amount of 1:10 dilution of original volume. The resulting chemically competent cell solution

was aliquoted into microcentrifuge tubes in volumes of 100µL. The aliquots were stored in -80 ºC.

During transformation, chemical competent cell aliquots were incubated on ice for 30 minutes in order to thaw. Then, either all of Gibson assembly reaction mixture or all of T4 Ligation reaction mixture was added to thawed chemical competent cells. In other words, about 100 ng of plasmid was added to thawed cells. Following addition of plasmid, the cells were incubated on ice for 20 minutes. Heat-shock was applied to cells at 42ºC for 45 seconds and cells were incubated on ice for 2 minutes. Then, 250 µL of LB without any antibiotics was added onto the cells and incubated at 37ºC, 200 rpm for 45-60 minutes. After incubation cells were pelleted at 8000 rpm for 5 minutes and some amount of supernatant was removed. The cells were resuspended with the remaining supernatant and spread onto LB-Agar (recipe given in Appendix E, Table E.1) with appropriate antibiotics and incubated at 37ºC, overnight.

2.2. Construction of Plasmids

Initially, pZa tetO CsgA-SpyTag plasmid construction was done. *csgA* was first amplified using cgA pBD FWD and ZK021 using Q5 DNA polymerase. Then, the resulting PCR product was further amplified with cgA pBD FWD and ZK022 primer pair. One more round of amplification of the last PCR product was conducted using cgA pBD FWD and ZK023 primer pair. The last PCR product was loaded in 1% agarose gel containing SYBR™ Safe DNA gel stain and electrophoresis was conducted at 130V for 30 minutes. Resulting linearized DNA extract and pZa vector were digested by MluI (NEB) and KpnI (NEB) enzymes. Digested fragments were further verified on 1% agarose gel. The expected band of csgA-SpyTag and pZa vector on agarose gel were cut out and DNA extraction from agarose gel was

conducted using NucleoSpin Gel and PCR Clean-up kit (Macherey-Nagel). Digested DNA fragments were ligated by T4 DNA ligase (reaction recipe is given in Appendix E, Table E.10). The plasmid map is provided in Figure C.1. All of the ligation reaction mixture was transformed into chemically competent *E. coli* DH5α. Transformation was conducted as described above. Following overnight incubation, colonies were selected from LB-Agar plate and the ones positive for csgA-SpyTag were further verified by Sanger Sequencing (Genewiz, USA). Sequencing results were analyzed by Geneious Prime® (2021.1.1) software and resulting alignment is given in Figure D.1. The verified colonies were inoculated in 10 ml fresh LB medium with corresponding antibiotic and incubated at 37ºC, 200 rpm overnight. The inoculated cells were then used for preparing -80ºC cell stocks.

For construction of pET22b-SpyCatcher-YlmD plasmid, pET22b vector and YlmD were amplified with GO30, CK42 primers and GO28, GO29 primers, respectively in order to add overhang regions for Gibson assembly. The PCR was performed using Q5 DNA polymerase with recommended conditions set by the manufacturer. The PCR products were loaded in 1% agarose gel containing SYBR™ Safe DNA gel stain and electrophoresis was conducted at 130V for 30 minutes. The expected bands of corresponding pET22b-SpyCatcher vector and YlmD on agarose gel were cut out and DNA extraction from agarose gel was conducted using NucleoSpin Gel and PCR Clean-up kit (Macherey-Nagel) following the manufacturer's instructions. Resulting DNA extracts of pET22b-SpyCatcher vector and YlmD were assembled together via Gibson assembly reaction at 50ºC for 1 hour. The combination condition of pET22b-SpyCatcher vector and YlmD in Gibson assembly mixture was adjusted as 1:6 molar ratio respectively. The plasmid map is provided in Figure C.2. Once the incubation

was over, all of the Gibson assembly reaction mixture was transformed into chemically competent *E. coli* DH5α strain. Transformation was conducted as described above. Following overnight incubation, colonies were selected from LB-Agar plate and the ones containing laccase gene were further verified by Sanger Sequencing (Genewiz, USA). Sequencing results were analyzed by Geneious Prime® (2021.1.1) software and resulting alignment is given in Figure D.2. The verified colonies were inoculated in 10 ml fresh LB medium with corresponding antibiotic and incubated at 37ºC, 200 rpm overnight. The inoculated cells were then used for preparing -80ºC cell stocks.

In order construct pET22b SpyCatcher-CotA plasmid, pET22b vector and CotA were amplified with GO30, CK42 primers and GO31, GO32 primers, respectively in order to add overhang regions for Gibson assembly. The PCR was performed using Q5 DNA polymerase with recommended conditions set by the manufacturer. The PCR products were loaded in 1% agarose gel containing SYBR™ Safe DNA gel stain and electrophoresis was conducted at 130V for 30 minutes. The expected bands of corresponding pET22b-SpyCatcher vector and CotA on agarose gel were cut out and DNA extraction from agarose gel was conducted using NucleoSpin Gel and PCR Clean-up kit (Macherey-Nagel) following the manufacturer's instructions. Resulting DNA extracts of pET22b-SpyCatcher vector and CotA were assembled together via Gibson assembly reaction at 50ºC for 1 hour. The combination condition of pET22b SpyCatcher vector and CotA in Gibson assembly mixture was adjusted as 1:3 molar ratio respectively. The plasmid map is provided in Figure C.3. Once the incubation was over, all of the Gibson assembly reaction mixture was transformed into chemically competent *E. coli* DH5α strain. Transformation was conducted as

described above. Following overnight incubation, colonies were selected from LB-Agar plate and the ones containing laccase gene were further verified by Sanger Sequencing (Genewiz, USA). Sequencing results were analyzed by Geneious Prime® (2021.1.1) software and resulting alignment is given in Figure D.3. The verified colonies were inoculated in 10 ml fresh LB medium with corresponding antibiotic and incubated at 37ºC, 200 rpm overnight. The inoculated cells were then used for preparing -80ºC cell stocks.

Last of all, for construction of pET22b SpyCatcher-GRFT plasmid, pET22b vector, SpyCatcher and GRFT were amplified with GO23, CK42 primers, GO20, GO21 primers, and pREA145, GO22 primers respectively in order to add overhang regions for Gibson assembly. The PCR was performed using Q5 DNA polymerase with recommended conditions set by the manufacturer. The PCR products were loaded in 1% agarose gel containing SYBR™ Safe DNA gel stain and electrophoresis was conducted at 130V for 30 minutes. The expected bands of corresponding pET22b vector, SpyCatcher and GRFT on agarose gel were cut out and DNA extraction from agarose gel was conducted using NucleoSpin Gel and PCR Clean-up kit (Macherey-Nagel) following the manufacturer's instructions. Resulting DNA extracts of pET22b vector, SpyCatcher and GRFT were assembled together via Gibson assembly reaction at 50ºC for 1 hour. The combination condition of pET22b vector, SpyCatcher and GRFT in Gibson assembly mixture was adjusted as 1:4:4 molar ratio respectively. The plasmid map is provided in Figure C.4. Once the incubation was over, all of the Gibson assembly reaction mixture was transformed into chemically competent *E. coli* DH5α strain. Transformation was conducted as described above. Following overnight incubation, colonies were selected from LB-Agar plate and the

ones containing laccase gene were further verified by Sanger Sequencing (Genewiz, USA). Sequencing results were analyzed by Geneious Prime® (2021.1.1) software and resulting alignment is given in Figure D.4. The verified colonies were inoculated in 10 ml fresh LB medium with corresponding antibiotic and incubated at 37ºC, 200 rpm overnight. The inoculated cells were then used for preparing -80ºC cell stocks. All the plasmid designs were constructed in Benchling online tool and the molar concentration of vectors and inserts were calculated using NEBioCalculator®.

The sequences of all aforementioned gene fragments and primer pairs are given in Table A.1 and Table B.1, respectively.

2.3. Sanger Sequencing and Sequence Alignments

Once the clonings of each construct were finished, inoculated colonies were used for plasmid isolation using Thermo Scientific GeneJet Plasmid Miniprep Kit following the instructions provided by the manufacturer. The isolated plasmid was measured for concentration using Thermo Scientific NanoDrop™ 2000 Spectrophotometer. According to the measured concentration, 1000 ng of plasmid was prepared for sequencing by mixing it with 5 µL of 5 µM sequencing primer and adding up the final volume to 15 µL with dH_2O. Then, samples were sent to Genewiz (USA) for Sanger Sequencing. Results were downloaded from Genewiz website in. ab1 format and designed plasmid maps were downloaded in .gb file format from Benchling online tool for alignment purposes using Geneious Prime® (2021.1.1) software.

2.4. Expression of Functionalized Biofilm Proteins

In order to induce biofilm protein formation, first pZa tetO CsgA-SpyTag plasmid was transformed into ΔcsgA competent cells via chemical transformation. Colonies containing the plasmid construct were inoculated into fresh LB medium supplied with appropriate antibiotics and grown overnight at 37°C, 200 rpm. Following overnight incubation, the cells were diluted 1:100 into fresh LB medium with appropriate antibiotics and grown until OD_{600} reached 0.4. Once OD_{600} condition was achieved, the cells were pelleted at 8000xg for 5 minutes and supernatant was removed. The cell pellet was resuspended in fresh 1X M63 medium (recipe is given in Appendix E, Table E.2) supplied with $MgSO_4$ (Sigma) (1 mM), glycerol (Sigma) (0.2 %), casein hydrolysate (Sigma) (0.1 %) and thiamine (1 μg/mL). Next, the cells were induced with aTc to have a final concentration of 250 μg/mL. Following induction, cells were incubated in 30°C incubator in stationary condition. aTc was added every two days with the same concentration initial induction. The induction period was continued for 6 days. At the end of 6 days the cells were used for biofilm fiber purification.

2.5. Expression of Recombinant Proteins

In order to express recombinant proteins of SpyCatcher fused with YlmD and SpyCatcher fused with CotA, first pET22b SpyCatcher-YlmD and pET22b SpyCatcher-CotA plasmid constructs were transformed into *E. coli* BL21 (DE3) competent cells via chemical transformation. Following transformation, bacterial cells having the pET22b SpyCatcher-CotA and pET22b SpyCatcher-YlmD plasmids

were inoculated in fresh LB medium with appropriate antibiotics overnight at 37°C, 200 rpm. After overnight incubation, cells were diluted 1:100 into fresh LB medium supplied with appropriate antibiotics and 0.25 mM final concentration of $CuSO_4$ (Sigma). The cells were grown until OD_{600} reached up to 0.4 and they were induced with Isopropyl β-D-1-thiogalactopyranoside (IPTG) to have a final concentration of 1 mM. Next, the cells harboring pET22b SpyCatcher-YlmD plasmid were incubated at 37°C, 200 rpm overnight and cells harboring pET22b SpyCatcher-CotA plasmid were incubated at 18°C, 200 rpm overnight. After incubation, the cells were pelleted via centrifugation at 8000xg for 5 minutes and the supernatant was removed. The cells were then lysed and the resulting whole cell lysate was used for complex formation with functionalized biofilm protein, CsgA-SpyTag.

For expression of SpyCatcher-GRFT fusion protein, first pET22b SpyCatcher-GRFT plasmid construct was transformed into *E. coli* BL21 (DE3) competent cells via chemical transformation. Following transformation, bacterial cells having the mentioned plasmid construct were inoculated in fresh LB medium with appropriate antibiotics overnight at 37°C, 200 rpm. After overnight incubation, cells were diluted 1:100 into fresh LB medium supplied with appropriate antibiotics. The cells were grown until OD_{600} reached up to 0.4 and they were induced with Isopropyl β-D-1-thiogalactopyranoside (IPTG) to have a final concentration of 1 mM. Next, the cells were incubated at 16°C, 200 rpm overnight. After incubation, the cells were pelleted via centrifugation at 8000xg for 5 minutes and the supernatant was removed. The cells were then lysed and the resulting whole cell lysate was used for complex formation with functionalized biofilm protein, CsgA-SpyTag.

2.6. Biofilm Fiber Purification

Following the induction period of cells harvesting pZa tetO CsgA-SpyTag plasmid construct, biofilm fiber purification was done as described by Joshi et al [45]. At the end of incubation period, Gdn-HCl was added to the cultures to have a final concentration of 0.8 M and then incubated at 4°C for 2 hours. Following incubation, the cultures were filtered through a 47 mm polycarbonate filter membrane having 10 μm pores (EMD Millipore). The residue on the filter membrane was incubated with 5 mL of 8M Gdn-HCl for 5 minutes and vacuum filtered at the end of incubation period. Next, the filter membrane was rinsed with 5 mL dH_2O and vacuum filtered. The washing cycle was done for 3 rounds. The residue on the filter membrane was incubated with 5 mL of 5% (m/v) SDS for 5 minutes and then vacuum filtered. The membrane was rinsed with 5 mL of dH_2O and vacuum filtered. The washing cycle was done for 5 rounds. Next, the biofilm fibers on the filter membrane were collected with a spatula and the wet weight of the collected biofilm fibers were measured using a microbalance. The collected fibers were stored in -20°C for further use in complex formations with SpyCatcher containing fusion proteins.

2.7. Enzyme Activity Measurements

The enzyme activity of SpyCatcher fused with YlmD and SpyCatcher fused with CotA were done following growth and induction periods as described in Section 2.5. At the end of induction period the cells were pelleted at 8000xg for 5 minutes and the supernatant was removed. Afterwards, the pellet was resuspended in 1X Phosphate Buffer Saline (PBS, 137 mM NaCl, 2.7 mM KCl, 10 mM Na_2HPO_4, 1.8 mM KH_2PO_4) pH 7.0 at a dilution rate of 1:10 and Phenylmethylsulfonyl fluoride

(PMSF) was added to have a final concentration of 1 mM. Then, 3 rounds of freeze-thaw cycle were applied using liquid nitrogen and sonication was conducted for 5 minutes with 10 seconds ON and 10 seconds OFF cycles with an amplitude of 35%. Then, the sonicated cells were centrifuged at 13000xg for 45 minutes and the supernatant was filtered using a 0.20 μm pore size syringe filter. The resulting total protein mixture was used for enzyme activity measurement for SpyCatcher-YlmD and SpyCatcher-CotA fusion proteins following protein concentration measurement via Quick Start Bradford Protein Assay (Bio-Rad) as described by the manufacturer. The enzyme activity assay was conducted for measured total protein concentrations of 1500 μg/mL, 1000 μg/mL, 750 μg/mL, 500 μg/mL, 250 μg/mL, 125 μg/mL, 25 μg/mL, and 0 μg/mL. The enzyme activity measurement was conducted as described by Chandra et al [12]. Briefly 0.1 M sodium acetate buffer (pH 5.0) containing 5 mM 2,2'-azino-bis (3-ethylbenzothiazoline-6-sulfonic acid) (ABTS) was added to the wells containing SpyCatcher-YlmD and SpyCatcher-CotA and absorbance values were read at 420 nm with SpectraMax M5 Microplate Reader spectrophotometer (Molecular Devices). The measurements were taken at every 20 minutes for 2 hours at 37°C.

2.8. Congo Red (CR) Staining

Congo Red staining of SpyTag fused CsgA proteins was initiated as described in Section 2.4 adopted to growing and inducing cells coding for CsgA-SpyTag fusion proteins in 24 well plates. At the end of growth and induction periods, the cells in wells assigned for CR staining were resuspended by pipetting and transferred into 2 mL sample collection tubes. Then, the cells were pelleted at 8000xg for 5 minutes and the supernatant was removed. The cell pellet was washed with 1X PBS and

centrifuged at 8000xg for 5 minutes and the supernatant was removed. The washing cycle was for 2 rounds in total. Afterwards, the cells were incubated with 1 mg/mL CR for 30 minutes at room temperature. Following incubation, the samples were centrifuged at 14000xg for 3 minutes and the supernatant was used for absorbance measurement at 480 nm. In order to normalize the absorbance of CR, OD_{600} was also measured prior to CR staining. The normalization was done according to the – $[OD_{480}/OD_{600}]$ formulation.

2.9. SDS-PAGE and Western Blot

In order to verify production of recombinant proteins, CsgA-SpyTag and SpyTag – SpyCatcher complex formations SDS-PAGE and Western Blot techniques were used. Recombinant proteins, SpyCatcher-GRFT, SpyCatcher-YlmD and SpyCacther-CotA, were used subsequent to purification as explained in Section 2.5. Same concentrations of SpyCatcher-GRFT, SpyCatcher-YlmD, and SpyCacther-CotA samples were dissolved in 1X SDS loading dye (Laemmli Sample Buffer) and incubated at 95°C for 5 minutes prior to loading into the gel. CsgA-SpyTag samples and CsgA-SpyTag + SpyCatcher-GRFT/YlmD/CotA complex samples were incubated in 100% Hexafluoro isopropanol (HFIP) overnight in order to monomerize fibers into major curli subunit CsgA, since otherwise CsgA cannot be observed in SDS-PAGE [46]. Following overnight incubation, HFIP was allowed to volatilize in a chemical hood and the samples were further dried with nitrogen to remove all the HFIP. Then, the samples were dissolved in 2X SDS loading dye (Laemmli Sample Buffer) and incubated at 95°C for 5 minutes prior to loading into the gel.

To be able to observe CsgA-SpyTag and CsgA-SpyTag + SpyCatcher-GRFT/YlmD/CotA complexes 15% SDS resolving gel was used since the molecular

weights of the samples started from 14 kDa. The composition of the separating gel was consisted of 2.2 mL ddH_2O, 2.6 mL 1.5 M Tris-HCl (pH 8.8), 100 µL 10% (w/v) SDS, 5 mL Acrylamide/Bisacrylamide (30%/0.8% w/v), 100 µL 10% (w/v) APS, 10 µL tetramethylethylenediamine (TEMED). Stacking gel composition was prepared with 2.975 mL ddH_2O, 1.25 mL 0.5 M Tris-HCl (pH 6.8), 50 µL 10% (w/v) SDS, 0.67 mL Acrylamide/Bisacrylamide (30%/0.8% w/v), 50 µL 10% (w/v) APS, 5 µL TEMED. Following the loading of samples, the gel was run at 140V in 1X SDS Running Buffer. At the end, gels were stained with Coomassie staining solution (45% methanol, 10% acetic acid, 3 g/L Coomassie Brilliant Blue R-250). Following staining, the gels were destained in destaining buffer (30% methanol, 10% acetic acid) to remove the excess Coomassie Brilliant Blue on the gel.

To be able to verify the proteins via his-tag, Western Blot analysis was conducted. The proteins on the gel at the end of running step, were transferred to a Polyvinylidene fluoride (PVDF) membrane (Thermo Scientific). Transfer process was conducted with the help of Transblot Transfer System (Biorad) using Turbo run option in 7 minutes. At the end of the transfer, PVDF membrane was incubated with 5% milk powder dissolved in 1X TBST at 4°C overnight on a shaker for blocking. Following blocking, PVDF membrane was incubated with anti-his primary antibody solution prepared with 1X TBST with a dilution rate of 1:5000, for 1 hour at room temperature using a shaker. At the end of 1 hour, the PVDF membrane was washed with 1X TBST for 5, 10, 10 minutes respectively using a shaker. Then, the membrane was incubated with anti-mouse secondary antibody conjugated with horseradish peroxidase (HRP) dissolved in 1X TBST with a dilution rate of 1:10000 for 1 hour at room temperature on a shaker. Then, the membrane was washed with

1X TBST for 5, 10, 10 minutes respectively. At the end, the membrane was visualized after 2 minutes of incubating with ECL substrate (Biorad) as described by the manufacturer using Fusion® Software of Vilber Lourmat imaging system.

2.10. Transmission Electron Microscopy (TEM) and Focused Ion Beam (FIB) Imaging

In order to verify CsgA-SpyTag fiber formation by TEM, the purified CsgA-SpyTag fiber pellets were resuspended with ddH_2O to have a final concentration of 1 mg/mL. 30 µL droplets containing CsgA-SpyTag fibers were dropped on parafilm to be able to maintain the droplet form. Formvar-Carbon coated TEM grids (200 mesh nickel grids, Electron Microscopy Sciences) were placed on top of the droplets and incubated for 5 minutes. Then, TEM grids were washed with 30 µl ddH_2O and 30 µL selective binding buffer (1X PBS, 300 mM NaCl, 80 mM imidazole, 0.2% (v/v) Tween-20) for 5 minutes each, respectively. Then, the grids were placed on top of 90 µL 10 nM 5 nm Ni-NTA gold nanoparticles dissolved in selective binding buffer and incubated in dark for 90 minutes at room temperature. Following incubation, TEM grids were washed with 30 µL selective binding buffer 5 times, 30 µL PBS 2 times, and 30 µL ddH_2O 2 times for 5 minutes each, respectively. Finally, TEM grids were incubated on 30 µL 2% uranyl acetate (UA) droplets for 25 seconds and left for drying at room temperature. The grids were then visualized with 200kV TEM (FEI Tecnai).

For verification of SARS-CoV-2 capture by CsgA-SpyTag + SpyCatcher-GRFT complex TEM was also used. The samples of SARS-CoV-2 mixed and incubated

with CsgA-SpyTag + SpyCatcher-GRFT complex were dropped on Formvar-Carbon TEM grids and left for drying overnight in Biosafety cabinet. Air drying the droplets led the inactivation of SARS-CoV-2 in the samples without disturbing its physical state. Afterwards, the grids with samples were washed with 30 µL dH_2O once, stained with 30 µL 2% uranyl acetate (UA) for 25 seconds and left for drying at room temperature in biosafety cabinet. The grids were then visualized with 200 kV TEM (FEI Tecnai).

Another imaging for demonstrating SARS-CoV-2 capture by CsgA-SpyTag + SpyCatcher-GRFT complex was by Focused Ion Beam, which is very similar to Scanning Electron Microscope (SEM), but has higher resolution. The samples of SARS-CoV-2 mixed and incubated with CsgA-SpyTag + SpyCatcher-GRFT complex were dropped on silica wafers and left for drying overnight in Biosafety cabinet. Air drying the droplets led the inactivation of SARS-CoV-2 in the samples without disturbing its physical state. Later, the silica wafers were attached to stubs with carbon tape. The samples were then coated with Au/Pd of 10 nm thickness using Precision Etching and Coating System (PECS) since the samples were not conductive in their natural states. Finally, the samples were visualized in SEM/FIB (FEI Nova NanoLab 600i SEM/FIB).

2.11. SpyTag – SpyCatcher Complex Formation

In order to form SpyTag – SpyCatcher complexes with CsgA-SpyTag, SpyCatcher-YlmD, SpyCatcher-CotA and SpyCatcher-GRFT, fusion proteins were purified as described in previous parts. The complex formation was carried out in 50 mM Phosphate Buffer (1 M KH_2PO_4, 1 M K_2HPO_4) pH 7.2 [45]. CsgA-SpyTag was

incubated with SpyCatcher-GRFT or SpyCatcher-YlmD or SpyCatcher-CotA in phosphate buffer at 4°C, overnight. The samples were collected at the end of incubation period by centrifuging at 14000xg for 5 minutes in order to remove the supernatant from the CsgA-SpyTag + SpyCatcher complex. The CsgA-SpyTag – SpyCatcher-GRFT/YlmD/CotA complexes in fiber form were isolated from the supernatant and then used for further analysis.

2.12. Degradation of Ciprofloxacin with CsgA-SpyTag – SpyCatcher-CotA/YlmD Complexes and LCMS QTOF Analysis

The degradation experiments of Ciprofloxacin were done once the CsgA-SpyTag - SpyCatcher-YlmD and CsgA-SpyTag - SpyCatcher-CotA complexes were formed as described in Section 2.11. Ciprofloxacin was then added on top the fiber complexes at a concentration of 10 μg/L and incubated at 37°C, for a specified time period. At the end of incubation, the samples were centrifuged at 14000xg for 5 minutes in order to pellet the fiber complex and remove the supernatant for analysis using Liquid Chromatography Mass Spectrometry Quadrupole Time of Flight (LC-MS QTOF). The supernatant was analyzed to check the presence of degradation products which occurred as a result of Ciprofloxacin degradation due to the fiber complexes of CsgA-SpyTag + SpyCatcher-YlmD and CsgA-SpyTag + SpyCatcher-CotA. The samples were transferred into LC-MS QTOF vials and they were analyzed in Agilent LC-MS QTOF 6530. The analysis was conducted without a column and the operating conditions were as following: 300°C for Gas Temperature, 8 L/min for Drying Gas Flow, 35 psi for Nebulizer, 250°C for Sheath Gas Temperature, 6 L/min for Sheath Gas Flow, 3500 V for capillary voltage (Vcap), and 170 V for fragmentor voltage. The analysis was conducted for positive ions.

2.13. SARS-CoV-2 Experiments for CsgA-SpyTag + SpyCatcher-GRFT

All infectivity assays with SARS-CoV-2 were performed in Biosafety Level 3 plus (BSL-3+) laboratory at Ankara University. To elucidate binding capacity of GRFT to SARS-CoV-2 ($TCID_{50} = 10^{7.25}$/mL) virus particles in a suspension, three different concentrations of SpyCatcher-GRFT in three different CsgA-SpyTag + SpyCatcher-GRFT complexes were mixed and incubated with the equal volume of the virus for 30 and 60 minutes. The mixtures were centrifugated (14000xg at 4°C) at each timepoint for 10 minutes. Supernatants were then transferred into sterile tubes and titrated in vitro for the infectivity. The remaining pellets in each tube were used for electron microscopy.

2.14. Protein Concentration Measurement via Western Blot for SpyCatcher-CotA, SpyCatcher-YlmD and SpyCatcher-GRFT

Protein concentration of SpyCatcher fused CotA, YlmD and GRFT proteins were calculated by Western Blot analysis. A calibration curve was formed using 5 different concentrations of N protein with stock concentration of 1.83 mg/mL. The calibration curve included 50 μg/mL, 100 μg/mL, 250 μg/mL, and 500 μg/mL of N protein diluted in autoclaved dH_2O. The fusion proteins of concern were used as different volumetric dilutions from the soluble part of whole-cell lysate in the experiments. The volumetric ratios were adopted to the sample volume of 20 μL when loading to SDS-PAGE gels. The Western blot protocol was the same as explained in Section 2.9. Once all the steps of incubations with primary and secondary antibodies and washing steps were completed the membrane was visualized in Fusion® Software of Vilber Lourmat. The “Quantification” tool of the

software was used to calculate the concentrations of the SpyCatcher fusion proteins. The software converts the signals obtained from each band to a graph profile and by assigning the known concentrations of the N protein to the calibration curve, the software calculates the unknown concentrations of SpyCatcher-CotA, SpyCatcher-YlmD and SpyCatcher-GRFT.

CHAPTER 3

RESULTS AND DISCUSSION

3.1. Cloning and Expression of Enzyme Fused SpyCatcher Proteins

In order to form the SpyTag-SpyCatcher complexes where SpyTag is fused to CsgA and SpyCatcher is fused to 2 types of laccase enzymes separately, the cloning of enzyme fused SpyCatcher was done in the beginning.

The cloning of *ylmD* and *cotA* genes into pET22b (+) vector were done simultaneously. Since both YlmD and CotA are proteins of *Bacillus subtilis* strain 168, they were amplified from the genomic DNA of *B. subtilis* strain 168 using the primers given in Table B.1 with overhangs suitable for pET22b (+) vector. The vector backbone was also amplified with the primers listed in Table B.1 with overhang regions corresponding to YlmD and CotA separately suitable for Gibson assembly. YlmD and CotA were fused to SpyCatcher domain with a GS linker in between to provide a flexible connection to the proteins. Histidine tags were added to C terminal of both fusion proteins as shown in Figure 3.

A.

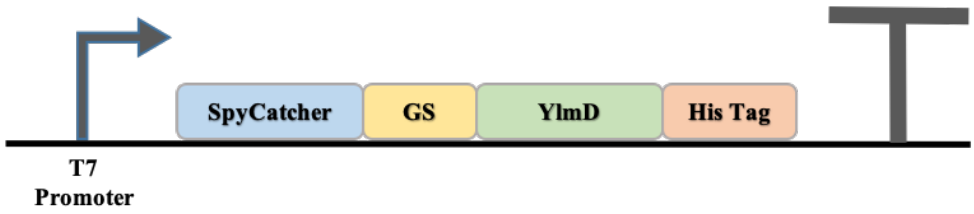

B.

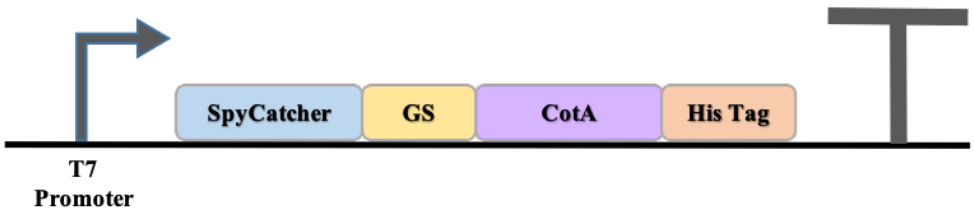

Figure 3. Schematic representation of A. SpyCatcher-YlmD and B. SpyCaycther-CotA fusion proteins expressing constructs. For both of the constructs there exists His tag at C terminal of fusion proteins and a GS linker in between SpyCatcher protein domain and YlmD and CotA separately.

The *cotA* and *ylmD* genes (Figure 4.A) and pET22b (+) vector backbone (Figure 4.B) were amplified via PCR using Q5 DNA polymerase. Following agarose gel electrophoresis and gel extraction they were cloned into pET22b (+) via Gibson assembly.

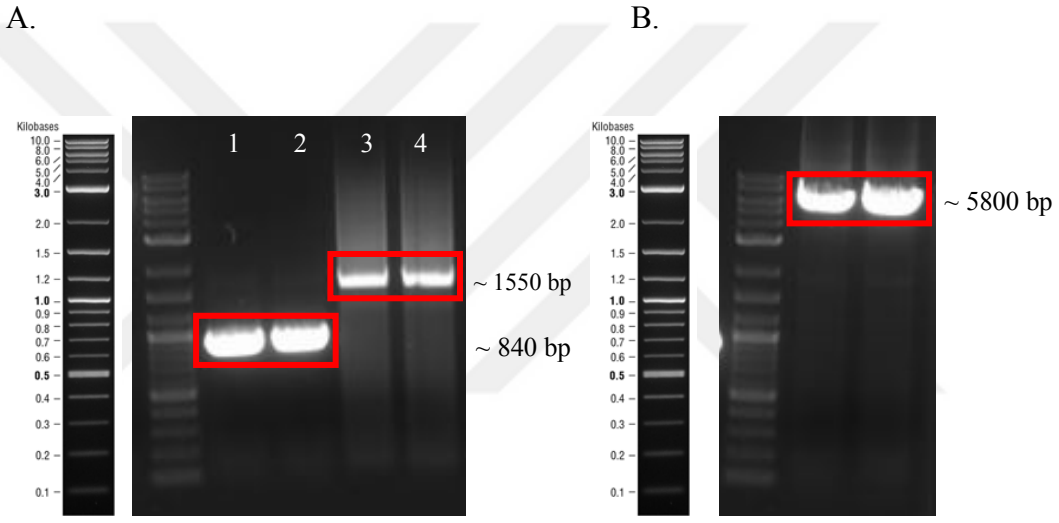

Figure 4. Cloning of ylmD and cotA genes to pET22b (+) vector. A. Agarose gel electrophoresis results of PCR amplified ylmD (lanes 1 and 2) and cotA (lanes 3 and 4) from genomic DNA of B. subtilis strain 168. B. Agarose gel electrophoresis result of PCR amplified pET22b (+) vector backbone. Both the genes and the vector backbone were amplified to have overhang regions suitable for each other for Gibson assembly cloning.

pET22b SpyCatcher-YlmD and pET22b SpyCatcher-CotA clonings were subsequently verified by both colony PCR using Pfu Polymerase and Sanger Sequencing (Figure D.2, and Figure D.3 respectively) with the plasmids isolated from positive colonies obtained by colony PCR (Figure 5).

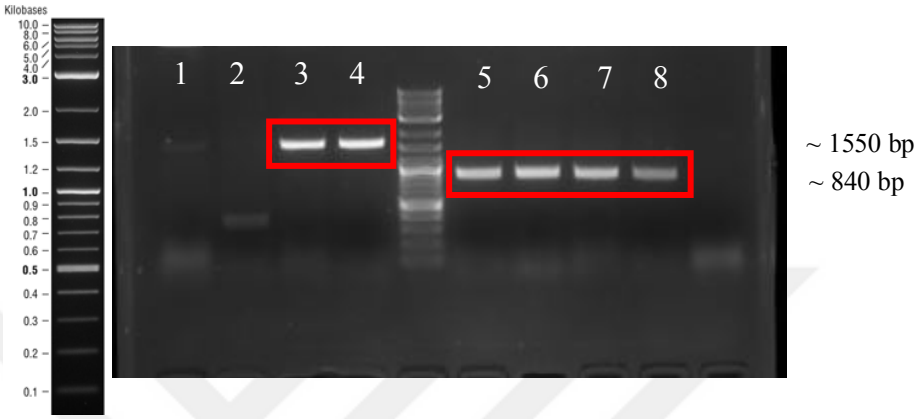

Figure 5. Colony PCR verification of pET22b SpyCatcher-YlmD (Lanes 3 &4) and pET22b SpyCatcher-CotA (Lanes 5, 6, 7 & 8) using Pfu polymerase. Colony PCR was conducted with the primers previously used for cloning of both pET SpyCatcher-YlmD and pET22b SpyCatcher-CotA constructs. Lanes 1, 2, 3 and 4 represent colonies 1-4 selected for pET SpyCatcher-YlmD and Lanes 5, 6, 7 and 8 represent colonies 1-4 selected for pET22b SpyCatcher-CotA.

Following Sanger Sequence verification of plasmids pET22b SpyCatcher-YlmD and pET22b SpyCatcher-CotA, they were chemically transformed into *E. coli* BL21 DE3 competent cells for high yield protein production upon induction. In order to obtain SpyCatcher-YlmD and SpyCatcher-CotA fusion proteins, the cells were induced with 1 mM IPTG in LB medium after they reached an OD_{600} of 0.4 for 24 hours at 37°C and 18°C, respectively at 200 rpm. Following induction, the cells were pelleted and lysed by freeze-thaw cycles using liquid nitrogen and then purified with

immobilized metal affinity chromatography (IMAC). However, the obtained eluate concentrations after IMAC were relatively low that we could not use them for further steps of experiments. Therefore, we decided to use soluble portion of whole cell lysate for SpyCatcher-YlmD and SpyCatcher-CotA fusion proteins for the upcoming experiment set-ups. Soluble parts of whole cell lysates were then checked for the fusion proteins with SDS-PAGE (Figure 6.A) and Western Blot (Figure 6.B) using antibodies against multiple Histidine tag.

A. B.

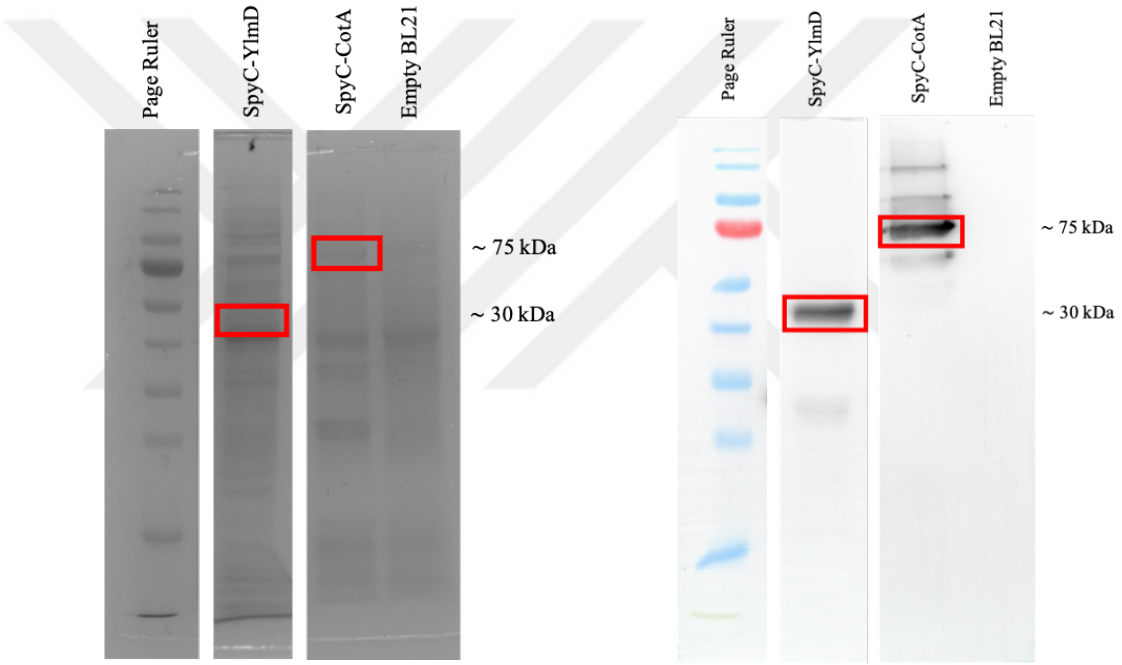

Figure 6. SDS-PAGE and Western Blot verification of SpyCatcher-CotA and SpyCatcher-YlmD fusion proteins. A. SDS-PAGE image of SpyCatcher-CotA and SpyCatcher-YlmD. First lane stands for Page Ruler ladder, second lane is SpyCacther-YlmD fusion protein (~ 30 kDa), third lane is for SpyCacther-CotA fusion protein (~ 75 kDa) and forth lane is for BL21 cells which do not contain either of pET22b SpyCatcher-CotA and pET22b SpyCatcher-YlmD plasmids. B. Western Blot image of SpyCatcher-CotA and SpyCatcher-YlmD. First lane stands for Page Ruler ladder, second lane is SpyCacther-YlmD fusion protein (~ 30 kDa), third lane is for SpyCacther-CotA fusion protein (~ 75 kDa) and forth lane is for BL21 cells

which do not contain either of pET22b SpyCatcher-CotA and pET22b SpyCatcher-YlmD plasmids.

3.2. Cloning and Expression of Griffithsin Fused SpyCatcher Protein

In order to form Griffithsin (GRFT) fused CsgA protein using SpyTag-SpyCatcher phenomenon, first Griffithsin was cloned to SpyCatcher domain via Gibson assembly method.

The cloning of *grft* and *spyC* genes into pET22b (+) vector was done simultaneously by both amplifying the genes and the pET22b backbone using the primers listed in Table B.1. Both *grft, spyC* and pET22b backbone were amplified with complementary overhang regions suitable for Gibson assembly. GRFT was fused to SpyCatcher domain with a GS linker in between to provide a flexible connection to the protein and Histidine tags were added to C terminal of fusion protein as shown in Figure 7.

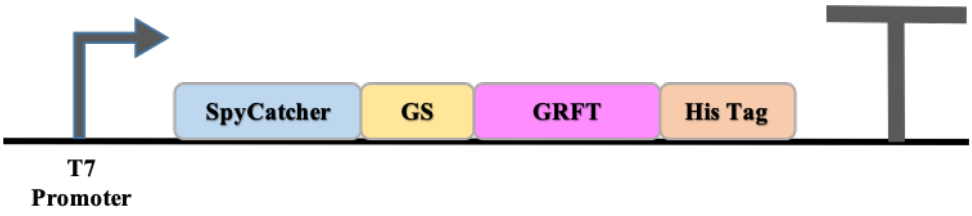

Figure 7. Schematic representation of SpyCaycther-Griffithsin fusion protein expressing construct. There exists a His tag at C terminal of SpyCatcher-GRFT fusion protein and a GS linker in between SpyCatcher protein domain and GRFT.

The amplification of *grft*, *spyC*, and pET22b (+) vector backbone were done separately by PCR using Q5 DNA polymerase. Following imaging of gene fragments on agarose gel electrophoresis and gel extraction, 2 inserts (Figure 8.A and Figure 8.B) were cloned into pET22b backbone (Figure 8.C).

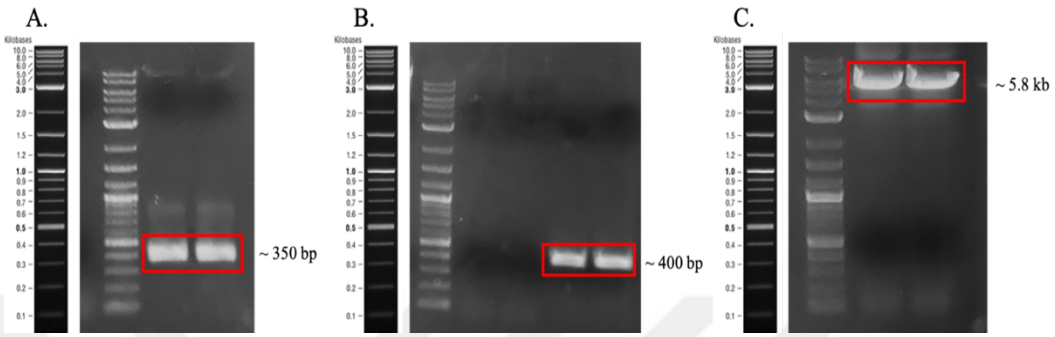

Figure 8. Agarose gel images for gene fragments of pET22b SpyCatcher-GRFT cloning. Agarose gel electrophoresis results of PCR amplified A. *spyC* gene fragment (~ 350 base pairs), B. *grft* (~ 400 base pairs), and C. pET22b backbone (~ 5800 base pairs). All of the gene fragments and pET22b backbone were PCR amplified with complementary overhang regions to each other and to the backbone. Gibson assembly was conducted with 2 inserts and pET22b backbone in 1 reaction mix. 1kb+ ladder was used.

The cloning of pET22b SpyCatcher-GRFT was verified with colony PCR using Pfu DNA polymerase for 4 randomly selected colonies. The colony PCR was conducted to verify SpyCatcher and GRFT separately using the primers that were used for PCR amplification of the corresponding gene fragments (Figure 9).

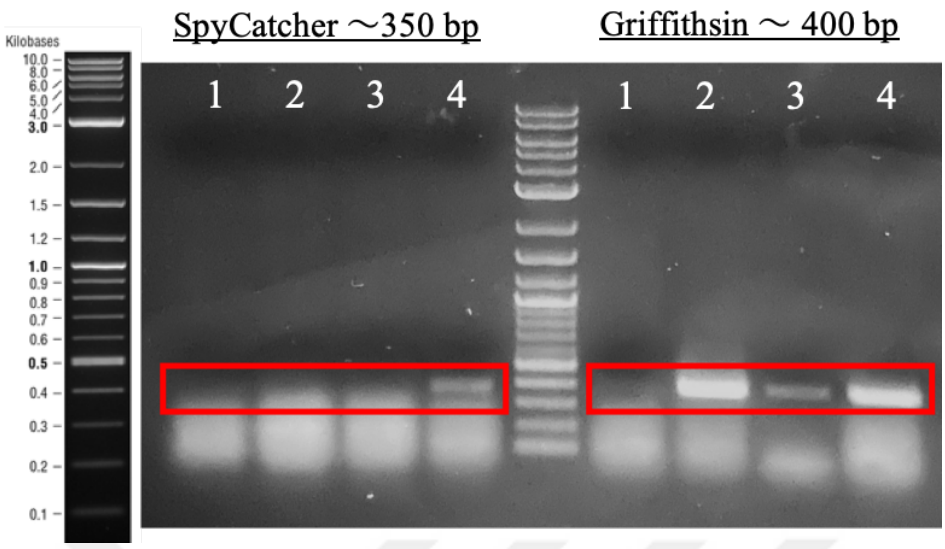

Figure 9. Colony PCR verification of pET22b SpyCatcher-GRFT using Pfu polymerase. Colony PCR was conducted with the primers previously used for cloning of pET22b SpyCatcher-GRFT construct. Lanes 1, 2, 3 and 4 represent colonies 1-4 selected for pET SpyCatcher-GRFT. Left side of the 1kb+ ladder represents colony PCR results of randomly selected 4 colonies for SpyCatcher presence and right side of the ladder represents colony PCR results of the same randomly selected 4 colonies for GRFT. Both of the inserts were checked since the cloning of SpyCatcher and GRFT into pET22b backbone took place simultaneously.

Once the results of colony PCR was evaluated, 4th colony was observed to have both SpyCatcher and GRFT as inserts. Therefore, the plasmid obtained from growth of 4th colony was sent for Sanger Sequence verification (Figure D.4).

Following Sanger sequencing, pET22b SpyCatcher-GRFT plasmid was transformed into *E. coli* BL21 DE3 cells for better yield of protein production upon induction with IPTG. In order to have SpyCatcher-GRFT fusion protein, cells were grown until OD_{600} of 0.4 in LB media at 16°C, 200 rpm for 24 hours. Following induction period, the cells were pelleted and lysed by freeze-thaw cycles using liquid nitrogen and then purified with immobilized metal affinity chromatography (IMAC).

However, the obtained eluate concentrations after purification were relatively low that they were not suitable for use in further steps of experiments. As a result, we decided to use soluble portion of whole cell lysate for SpyCatcher-GRFT fusion protein for the upcoming experiments. Soluble part of whole cell lysate was then checked for the expression of fusion protein with SDS-PAGE (Figure 10.A) and Western Blot (Figure 10.B) using antibodies against Histidine tags.

A. B.

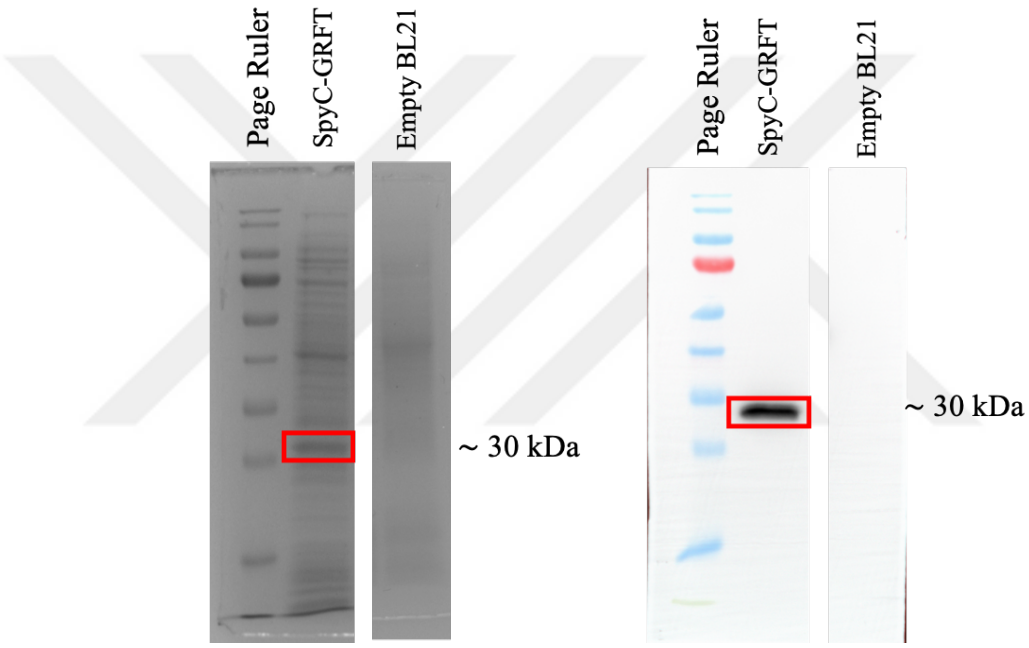

Figure 10. SDS-PAGE and Western Blot verification of SpyCatcher-GRFT fusion protein. A. SDS-PAGE image of SpyCatcher-GRFT. First lane stands for Page Ruler ladder, second lane is SpyCacther-GRFT fusion protein (~ 30 kDa), third lane is for BL21 cells which do not contain pET22b SpyCatcher-GRFT plasmid. B. Western Blot image of SpyCatcher-GRFT. First lane stands for Page Ruler ladder, second lane is SpyCacther-GRFT fusion protein (~ 30 kDa), third lane is for BL21 cells which do not contain either pET22b SpyCatcher-GRFT plasmid.

3.3. Cloning of SpyTag Fused Major Curli Biofilm Protein

In order to have a system of protein fused CsgA with the help of SpyTag-SpyCatcher couple, CsgA was fused with 13 amino acid long SpyTag protein tag.

The cloning of *spyT* to already existing *csgA* gene found in a pZa vector was conducted by a previous lab member. The cloning proceeded in such a way that, SpyTag was fused to CsgA domain by a series of PCR reactions using the primers listed in Table B.1. Initial step was the addition of GS linker site downstream of CsgA with 1 PCR setup. The next step was His-tag addition to downstream of GS linker with 1 round of PCR setup, which was then followed by addition of 13 amino acid SpyTag by 1 PCR setup (Figure 11).

Figure 11. Schematic representation of CsgA-SpyTag fusion protein expressing construct. There exists a His tag at C terminal of CsgA-SpyTag fusion protein and a GS linker in between CsgA protein domain and SpyTag for a flexible connection.

Following cloning, the pZa tetO CsgA-SpyTag construct was directly sent for Sanger sequence verification (Figure D.1). Following sequence verification, the selected colony was chemically transformed into *E. coli* ΔcsgA cells, which lack *csgA* gene in their genome. Therefore, production of CsgA-SpyTag fusion protein was solely depended on aTc induction, which activates the riboregulator system.

Further characterization of CsgA-SpyTag fusion protein was conducted by Congo Red (CR) Staining and Transmission Electron Microscopy (TEM) imaging, which will be explained in the next part.

3.4. Verification of Biofilm Formation by Congo Red (CR) Staining and Transmission Electron Microscopy (TEM)

Following cloning of pZa tetO CsgA-SpyTag, CsgA-SpyTag was checked for biofilm formation via Congo Red Staining with the purpose of quantifying amyloid proteins and Transmission Electron Microscopy (TEM) for imaging the structural properties of CsgA-SpyTag fusion biofilm protein.

CsgA, major curli biofilm protein, is an amyloid known for its β-sheet rich fibers. For amyloid structures such as CsgA, Congo Red is an amyloid binding type of dye, which can be used for quantification of amyloid structures [47]. In addition to CR Staining, TEM is used for visualization of biofilm proteins, which are expected to have fibrous, mash-like structures. Moreover, SpyTag fused biofilm proteins (CsgA) are labelled with Ni-NTA conjugated Au nanoparticles, which are known to interact with Histidine tags [48]. Therefore, with the help of Ni-NTA conjugated Au nanoparticles, visualization of SpyTag fused biofilm proteins (CsgA) are verified further since CsgA-SpyTag encoding plasmid was designed to have Histidine tags (Figure 11).

We have conducted CR Staining with 3 days old aTc induced cells encoding pZa pLtetO CsgA-SpyTag plasmid. The aim was to observe a change between CsgA-SpyTag protein production between ΔcsgA cells employing pZa pLtetO CsgA-SpyTag plasmid and ΔcsgA cells which lack any type of plasmid. The cell growth took place in M63 minimal media for 3 days, induction for biofilm formation was

done on the first day, and CR staining was conducted at the end of 3rd day as explained in Section 2.8. As a result of CR staining, biofilm formation was observed to be successfully achieved when compared to induced ΔcsgA cells, which were used as control group (Figure 12). Moreover, normalized quantification analysis of CsgA-SpyTag biofilm protein formation was conducted using [-OD_{480}/OD_{600}] formula which is shown in Figure 12.

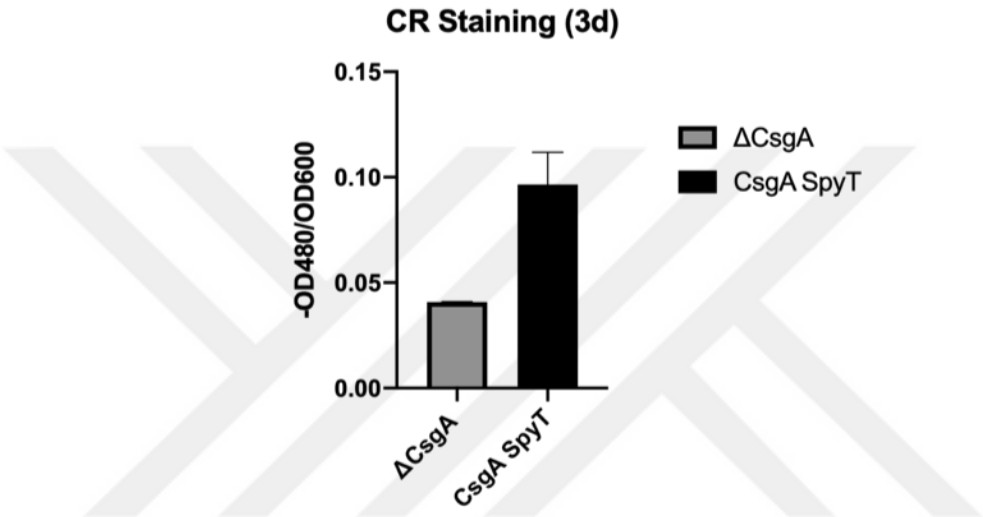

Figure 12. Congo Red Staining of cells obtained from 3 days of incubation in M63 media for ΔcsgA cells employing pZa pLtetO CsgA-SpyTag plasmid. ΔcsgA cells were used as control, n=3.

In addition to CR staining, TEM imaging was done for morphological verification of CsgA-SpyTag fusion protein. Induction and incubation step of CsgA-SpyT biofilm protein was conducted as explained in Section 2.4. Following 6 days of incubation/induction period CsgA-SpyTag biofilm protein purification through filtering was done according to the protocol given in Section 2.6. Finally, decellularized CsgA-SpyTag fibers obtained from purification were prepared for TEM imaging as explained in Section 2.10 and then visualized (Figure 13). TEM images indicated that filter purified CsgA-SpyTag fibers were in the form of biofilm protein structures, showing that fusion of SpyTag peptide did not cause a change in

morphology of CsgA structure as it was also observed in literature [49]. Moreover, the observed Ni-NTA conjugated Au nanoparticles attached to CsgA-SpyTag proteins verified the expression of CsgA-SpyTag with 6x Histidine tag was successful.

A. B.

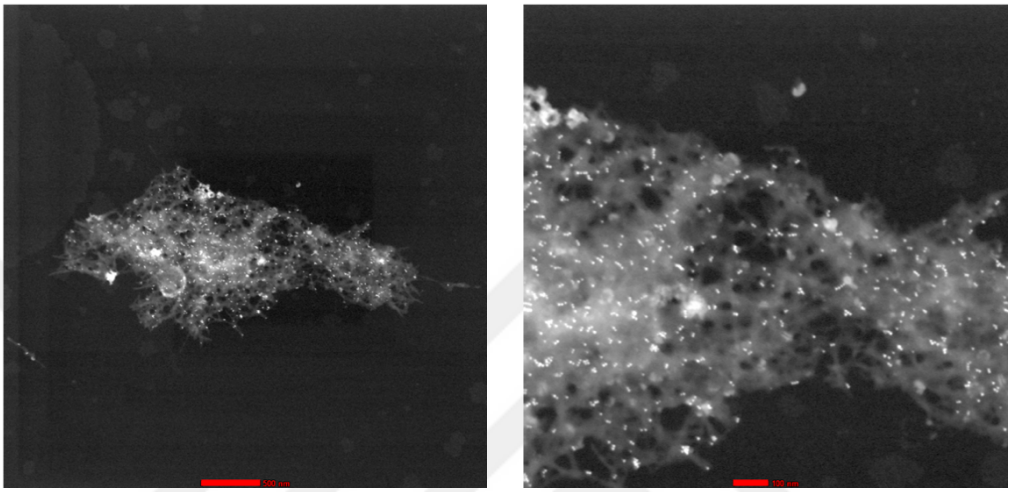

Figure 13. TEM images of CsgA-SpyTag purified biofilm protein. Filter purified CsgA-SpyTag samples were visualized with a scale bar of A. 500 nm and B. 100 nm. The samples were labelled with Ni-NTA conjugated Au nanoparticles.

3.5. Enzyme Activity Assay for Enzyme Fused SpyCatcher Proteins

Once the cloning of pET22b SpyCatcher-YlmD and pET22b SpyCatcher-CotA constructs were completed and the expressions were verified by SDS-PAGE and Western blot, the enzyme activity for SpyCatcher-YlmD and SpyCatcher-CotA fusion proteins was of interest. Since YlmD is a laccase domain protein and CotA is a verified laccase type protein, their enzyme activity is assessed through the absorbance change of ABTS substrate upon degradation in time [12].

E. coli BL21 DE3 cells employing pET22b SpyCatcher-YlmD and pET22b SpyCatcher-CotA constructs were grown in LB media and induced with 1 mM IPTG

at 37°C and 18°C respectively as explained in Section 2.5. At the end of induction period, the cells were pelleted and lysed as previously discussed in Section 2.7. We continued with protein purification using IMAC (immobilized metal affinity chromatography) techniques, however the obtained eluate protein concentration for both SpyCatcher-YlmD and SpyCatcher-CotA were relatively low that, we decided to continue enzyme activity measurement experiments with soluble whole cell protein fraction. First, protein concentration measurement assay for whole cell protein fraction was conducted with Quick Start Bradford Protein Assay (Bio-Rad). Then, enzyme activity measurement was performed for SpyCatcher-CotA and SpyCatcher-YlmD via ABTS assay as explained in Section 2.7. According to the protein concentration data obtained from Bradford Assay, I prepared a setup with 7 different concentrations of SpyCatcher-YlmD and SpyCatcher-CotA fusion proteins in 0.1 M sodium acetate buffer (pH 5.0) containing 5 mM ABTS (Figure 14). The assay was conducted by absorbance measurements for every 20 minutes during 120 minutes at 420 nm wavelength. The utilization of soluble whole cell protein fraction rather than purified protein might be interpreted as an unspecific approach, however the ABTS substrate is specific for laccase type enzymes. Moreover, the blank samples were whole cell protein fraction of induced empty *E. coli* BL21 DE3 cells, indicating that the expression of SpyCatcher-YlmD and SpyCatcher-CotA fusion proteins caused the observed change in substrate utilization.

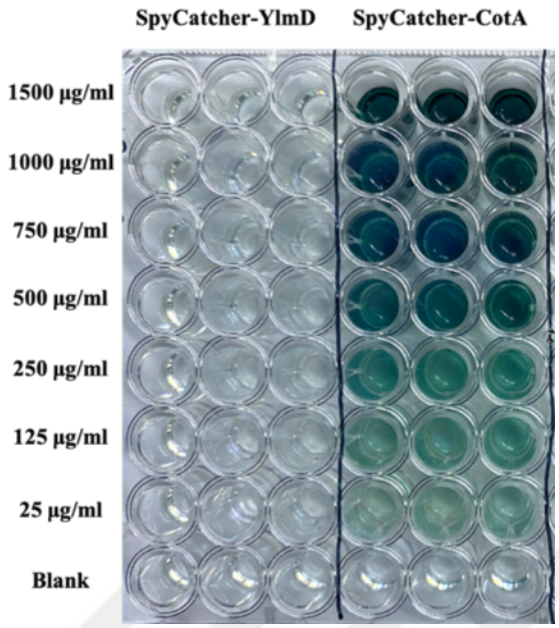

Figure 14. SpyCatcher-YlmD and SpyCatcher-CotA enzyme activity measurement. 96 well plate image of enzyme activity measurement setup of 7 different concentrations of fusion proteins at the end of 2 hours. Blank includes none of SpyCatcher-YlmD or SpyCatcher-CotA, n=3.

The data obtained from 2 hours of enzyme activity measurement was analyzed according to different whole cell protein concentrations with respect to time (Figure 15). It can be interpreted from the data that, the activity of SpyCatcher-CotA is significantly better than that of SpyCatcher-YlmD starting from the 20th minute for all seven concentrations. The trend for SpyCatcher-CotA during 2 hours of measurement interval, fits logarithmic curve for all concentrations, which can be clearly observed at higher concentrations. At lower concentrations the logarithmic trend is more clearly observed for CotA, whereas for SpyCatcher-YlmD logarithmic increase trend is not as obvious as SpyCatcher-CotA. On the other hand, different concentrations of SpyCatcher-YlmD was observed to have similar enzyme activity measurements during the measurement interval of 2 hours. Moreover, following 2 hours' time period a final absorbance measurement was taken at 24th hour in order to

observe the catalytic activity of SpyCatcher-YlmD and SpyCatcher-CotA fusion proteins. At 24th hour measurement, SpyCatcher-CotA was observed to have enzyme activity close to its measured values at the end of 2nd hour for the 4 highest concentration used in the experiment. For the rest of three relatively lower concentrations SpyCatcher-CotA did not exert enzyme activity as the aforementioned four highest concentrations. However, the measured values were higher than the measured values of initial 2 hours. Therefore, we concluded that SpyCatcher-CotA with initially high concentration reaches its maximum enzymatic activity within the initial 2 hours' time period. Similarly, the 24th hour enzymatic activity measurement of SpyCatcher-YlmD for the 4 highest concentrations were observed to be higher than the values measured in first 2 hours. For the last 3 lower concentrations, enzymatic activity of SpyCatcher-YlmD was observed to increase, however it was a slower increase when compared to the aforementioned 4 higher concentrations. For minimum concentration (25 μg/mL), no significant difference between Control and SpyCatcher-YlmD was observed, whereas the activity of SpyCatcher-CotA was reported to be significantly higher ($p < 0.0001$) than Control and SpyCatcher-YlmD. For the rest of the concentration values, catalytic activity of SpyCatcher-CotA was significantly better activity than both Control and SpyCatcher-YlmD. Therefore, we concluded that SpyCatcher-CotA has superior enzyme activity than SpyCatcher-YlmD for the given set of concentrations and for time intervals of 2 and 24 hours. Finally, we concluded that both SpyCatcher-CotA reaches a plateau for enzyme activity measurement representing its maximum enzyme activity for the corresponding concentrations. Therefore, for the experiments regarding Ciprofloxacin degradation, the time period of incubation was adjusted to be 2 hours.

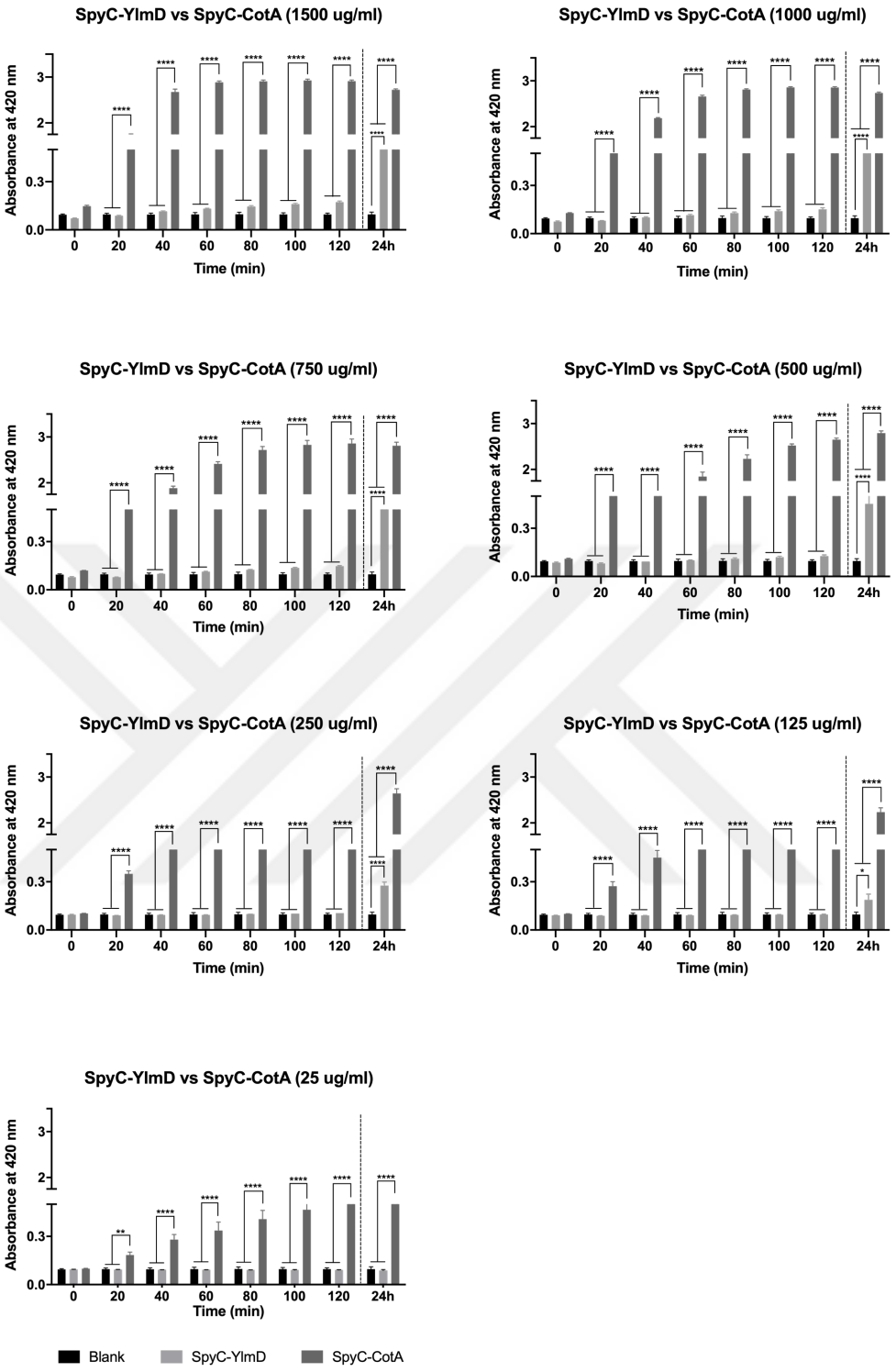

Figure 15. Enzyme activity measurements of SpyCatcher-YlmD and SpyCatcher-CotA for given concentrations during 2 hours of kinetic measurement and 24th hour measurement (Significance values were calculated by 2-Way ANOVA, $p < 0.0001$, n=3)

3.6. Verification of Enzyme Fused SpyTag - SpyCatcher Complex Formation

The complex formation between CsgA-SpyTag and SpyCatcher-CotA/YlmD fusion proteins was conducted following the verification of expression of CsgA-SpyTag and enzymatic activity of SpyCatcher-CotA, SpyCatcher-YlmD fusion proteins as shown in previous sections. The confirmation of complex formation between CsgA-SpyTag and enzyme fused SpyCatcher proteins was done through Western Blot analysis using a 12% SDS-PAGE gel.

Once the purifications of CsgA-SpyTag fibers and SpyCacther-CotA and SpyCatcher-YlmD fusion proteins were completed, complex formation reaction was set as explained in Section 2.11. As it can be interpreted form the Western blot data, complex formation between CsgA-SpyTag fibers and SpyCatcher fusion proteins can be observed by the increase in molecular weight of protein (Figure 16). We observed that the complex formation of SpyCatcher-CotA (~ 75 kDa), and SpyCatcher-YlmD (~ 45 kDa) fusion proteins with CsgA-SpyTag (~ 15 kDa) fibers took place as the samples prepared latter to the complex formation actually have higher molecular weights than the fusion proteins themselves. The CsgA-SpyTag + SpyCatcher-CotA was observed to be around 90 kDa, where SpyCatcher-CotA alone was observed to be 75 kDa, as expected. Likewise, CsgA-SpyTag + SpyCatcher-YlmD was observed at ~ 60 kDa with a very faint band whereas, SpyCatcher-YlmD had a band of ~ 45 kDa molecular weight. CsgA-SpyTag was also prepared for Western Blot as explained in Section 2.9, however it was not observed on the Western Blot. The last lane was reserved for whole cell lysate obtained from empty *E. coli* BL21 DE3 cells as control. Moreover, I expected to see the bands for CsgA-SpyTag and enzyme fused SpyCatcher proteins at the lanes of complexes, such as CsgA-SpyTag band, SpyCatcher-CotA band and CsgA-SpyTag + SpyCatcher-CotA complex band on the

lanes used for verification of complex formations (i.e. 3rd, 4th, 5th, 6th). However, the bands for CsgA-SpyTag, SpyCatcher-CotA and SpyCatcher-YlmD were not observed at the 3rd, 4th, 5th, and 6th lanes where the complex formations were actually occurred. The reason for this may be the low amount or short incubation period of HFIP that was used during sample preparation for Western blot.

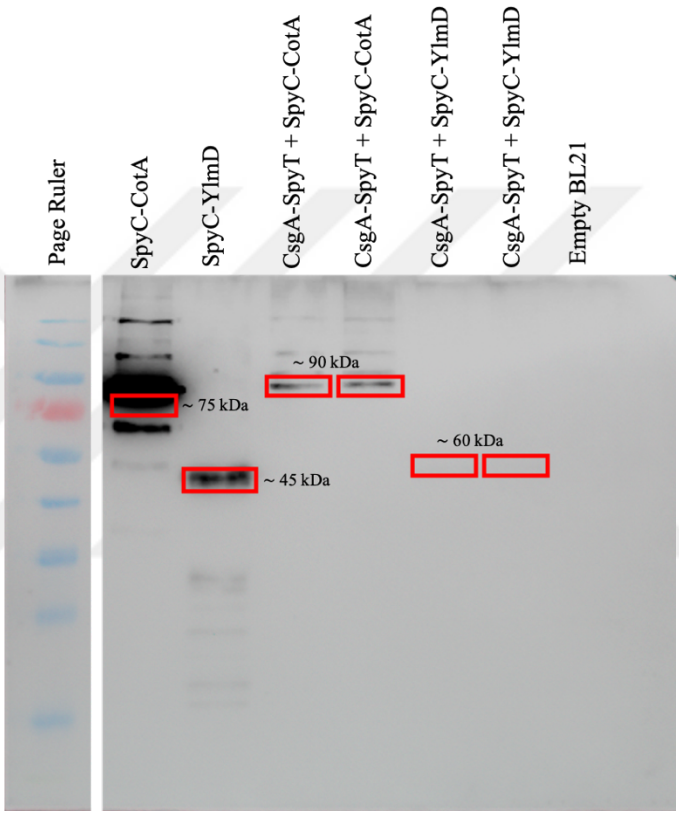

Figure 16. Western Blot data for verification of complex formation between CsgA-SpyTag and SpyCatcher-CotA, SpyCatcher-YlmD fusion proteins. Initial lane is Page Ruler. 2nd and 3rd lanes stand for SpyCatcher-CotA (~ 75 kDa) and SpyCatcher-YlmD (~ 45 kDa), respectively. 4th and 5th lanes represent CsgA-SpyTag + SpyCatcher-CotA complex with a band representing ~ 90 kDa. 6th and 7th lanes represent CsgA-SpyTag + SpyCatcher-YlmD complex with very faint band around 60 kDa. The last lane is for empty *E. coli* BL21 DE3 whole cell lysate.

3.7. Verification of Ciprofloxacin Degradation via LCMS-QTOF

The last step of CsgA-SpyTag complexed with enzyme fused SpyCatcher domain is to try them for degradation of Ciprofloxacin, which is the ultimate goal we aimed for CsgA-SpyTag complexed with laccase fused SpyCatcher. Laccases are known to degrade fluoroquinolone type antibiotics by attacking through the piperazine ring in their chemical structure. In earlier studies, degradation products of Ciprofloxacin were analyzed and characterized by Liquid Chromatography Mass Spectroscopy – Quadrupole Time of Flight (LCMS-QTOF) [23,25].

To do this, 3 different concentrations of CsgA-SpyTag + SpyCatcher-CotA/YlmD complexes were tested against constant Ciprofloxacin concentration of 10 μg/L. The Ciprofloxacin concentration was chosen to be 10 μg/L, because this amount represents concentrations of Ciprofloxacin that was encountered in most of the discharged wastewaters from hospitals and urban sources to sewage systems all around the world [50–54]. The ciprofloxacin concentrations measured in wastewaters of these countries show wide variations. The concentration of Ciprofloxacin measured in 2020 for 7 European countries with 13 different wastewater treatment plants' effluents showed maximum concentration close to 1μg/L [50], however in earlier studies in 2013, the measured concentrations were reported as high as 7 μg/L [52]. Therefore, the Ciprofloxacin concentration was chosen as 10 μg/L.

Three concentrations for both SpyCatcher-CotA and SpyCatcher-YlmD were used to form CsgA-SpyTag + SpyCatcher-CotA/YlmD complexes. 10 μg/L Ciprofloxacin was incubated with CsgA-SpyTag + SpyCatcher-CotA/YlmD complexes for 2 hours as previously explained in Section 3.5. Then the samples were analyzed for Ciprofloxacin degradation products using LCMS-QTOF (Figure 17).

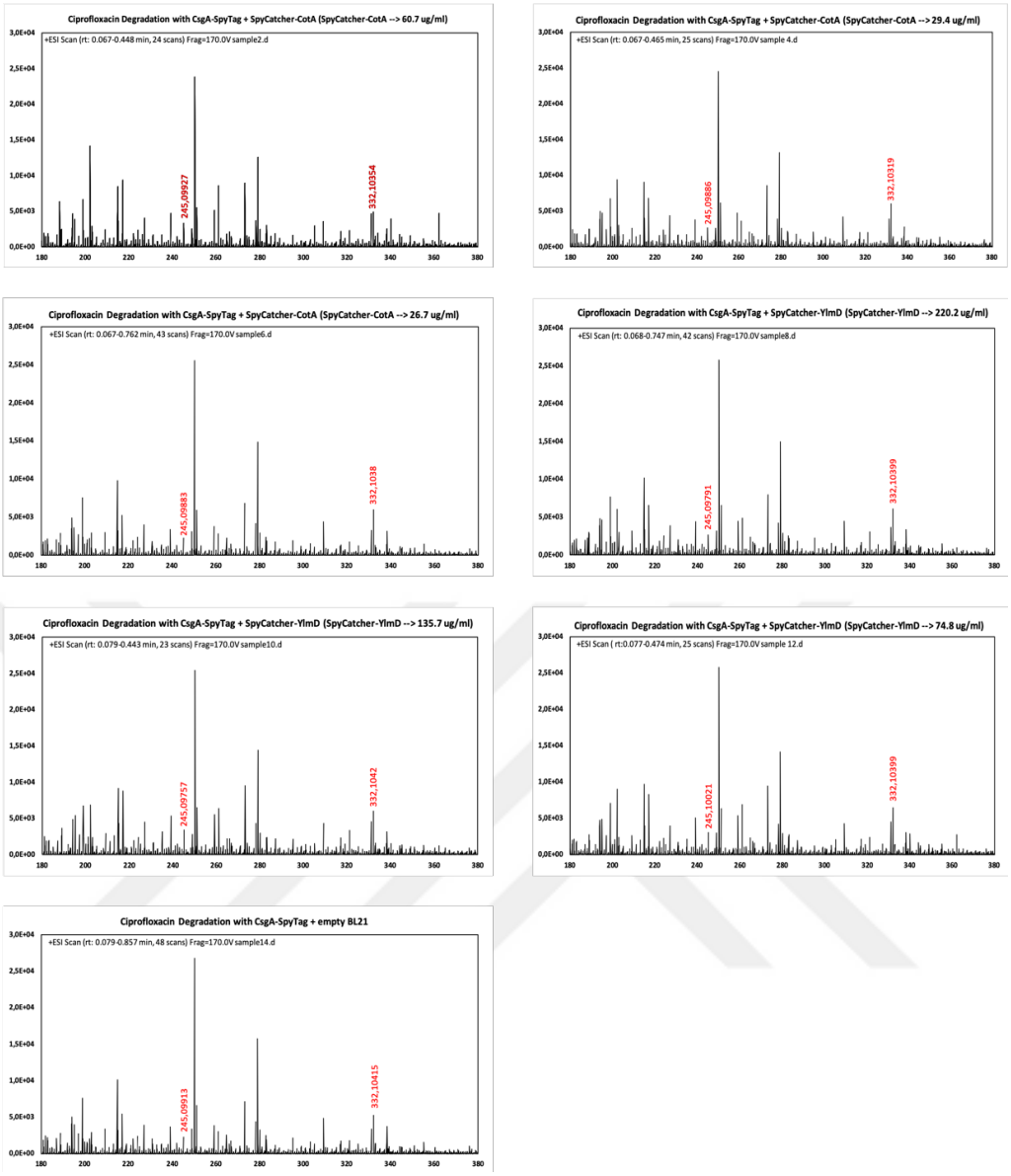

Figure 17. LCMS-QTOF analysis for Ciprofloxacin degradation products after incubation with CsgA-SpyTag + SpyCatcher-CotA/YlmD complexes formed with varying concentrations of SpyCatcher-CotA and SpyCatcher-YlmD.

The mass/charge (m/z) ratio for Ciprofloxacin analyzed at LCMS-QTOF is stated as 332 [25,55]. In the mass spectrums we obtained, we have also observed Ciprofloxacin signal. We have also observed some of the m/z values of Ciprofloxacin degradation products. However, one of the degradation products were observed to be more obvious than the others, which has m/z value of 245 and has a chemical formula of $C_{13}H_{12}N_2O_3$. Different from the chemical structure of Ciprofloxacin, this mentioned degradation product lacks the piperazine ring and the Fluorine group. Laccases are known to attack piperazinyl groups during oxidation reactions [24]. Therefore, we concluded that the laccases used in our constructs are capable of degrading Ciprofloxacin in 2 hours' time period. The degradation ratios of CsgA-SpyTag + SpyCatcher-CotA and CsgA-SpyTag + SpyCatcher-YlmD differ from each other. According to the data we obtained from mass spectroscopy, complexes with SpyCatcher-CotA were more effective in Ciprofloxacin degradation at the highest concentrations of both SpyCatcher fusion proteins, however at lower concentrations, however for subsequently lower concentrations SpyCatcher-YlmD showed better activity in degrading Ciprofloxacin that the formation of degradation product was observed to be higher. The occurrence of degradation product (m/z 245) after incubation with complexes formed with 60.7 μg/mL, 29.4 μg/mL and 26.7 μg/mL SpyCatcher-CotA, showed increase of 54.8%, 23.1% and 6.1%, respectively (Table 1). On the other hand, occurrence of the same degradation product (m/z 245) following incubation with complexes formed with 220.2 μg/mL, 135.7 μg/mL and 74.8 μg/mL SpyCatcher-YlmD, increased 21.6%, 57.9% and 41.9%, respectively. The increase in formation of the degradation product when 135.7 μg/mL SpyCatcher-YlmD was used in the complex formation was higher than that of 220.2 μg/mL SpyCatcher-YlmD. The reason may be due to the effect of high concentration

of SpyCatcher-YlmD that it effects the conformation of the protein in the complex structure. We also observed increase in degradation product formation in the samples where empty BL21 cell lysate was used, however the amount of increase was relatively lower.

Table 1. Increase in Ciprofloxacin degradation product formation with varying SpyCatcher-CotA and SpyCatcher-YlmD concentrations in complexes

	Concentration (µg/mL)	**Increase in Ciprofloxacin Degradation Product Formation (%)**
CsgA-SpyTag + SpyCatcher-CotA	26.7	6.1
	29.4	23.1
	60.7	54.8
CsgA-SpyTag + SpyCatcher-YlmD	74.8	41.9
	135.7	57.9
	220.2	21.6
CsgA-SpyTag + empty BL21	-	5.8

3.7.1. Concentration Determination for SpyCatcher-CotA & SpyCatcher-YlmD via Western Blot

The purification of recombinant proteins SpyCatcher-CotA and SpyCatcher-YlmD through IMAC columns did not yielded high concentrations. Therefore, I decided to integrate the SpyCatcher-CotA and SpyCatcher-YlmD fusion proteins as soluble part of whole cell lysate. As a result of this, the concentrations of fusion proteins used in

the experiments were calculated via Western Blot. In this indirect method of concentration determination, a calibration curve with a protein of known concentration which was purified using immobilized metal affinity chromatography (IMAC) against his-tag and checked for purity was generated. With the calibration curve formed, I compared the fusion proteins used in the Ciprofloxacin degradation experiment as explained in Section 2.14.

For SpyCatcher-CotA and SpyCatcher-YlmD, 3 different concentrations were used in the degradation experiment by arranging 3 different volumetric dilutions in the set-up. The volumetric dilutions were adjusted to be 8:10 (800 μL of fusion protein for 1000 μL reaction solution), 1:2 (500 μL of fusion protein for 1000 μL reaction solution) and 1:3 (333.3 μL of fusion protein for 1000 μL reaction solution). For both of the fusion proteins, the concentrations were analyzed using "Quantification" tool of Fusion® software by Vilber Lourmat Imaging System. The system separates each band and transfers the signal obtained from bands to graph profiles individually. Then, the system calculates the area under each curve and uses that information for comparing the area under the band representing the unknown proteins. As a result, by assigning known concentrations to the calibration curve, the unknown concentrations were calculated for both SpyCatcher-CotA and SpyCatcher-YlmD. For SpyCatcher-CotA, 3 different dilutions that were used in Ciprofloxacin degradation experiment, were analyzed and with the calibration curve obtained they were calculated to be 27 μg/mL, 30 μg/mL, and 60 μg/mL for SpyCatcher-CotA –1, SpyCatcher-CotA –2, and SpyCatcher-CotA –3, respectively (Figure 18).

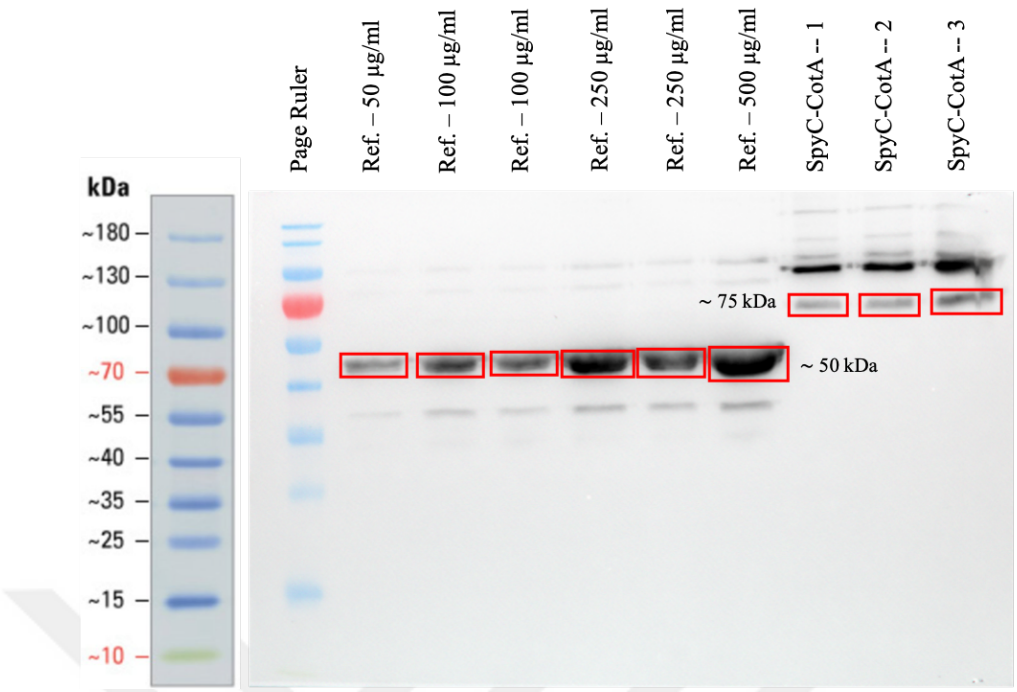

Figure 18. Western blot for concentration determination of different dilutions of SpyCatcher-CotA used in ciprofloxacin degradation experiment. Initial lane represents Page Ruler. Lanes from 2 to 7 stand for different concentrations of reference protein, i.e. 50 µg/mL, 100 µg/mL, 250 µg/mL, 500 µg/mL. Lanes 8, 9, and 10 are three different dilutions of SpyCatcher-CotA fusion protein that were used in the degradation experiment, which were calculated to be 27 µg/mL, 30 µg/mL, and 60 µg/mL, respectively. Fusion® software was used for all of the concentration analysis.

Moreover, for SpyCatcher-YlmD, 3 different dilutions that were used in Ciprofloxacin degradation experiment, were analyzed and with the calibration curve obtained they were calculated to be 75 µg/mL, 135 µg/mL, and 220 µg/mL for SpyCatcher-YlmD –1, SpyCatcher- YlmD –2, and SpyCatcher- YlmD –3, respectively (Figure 19).

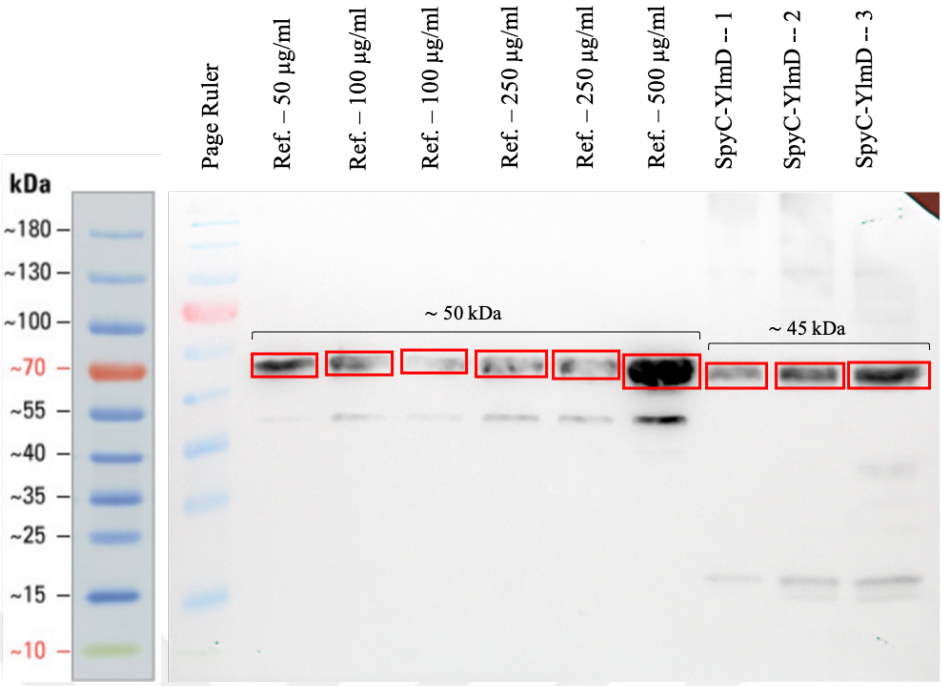

Figure 19. Western blot for concentration determination of different dilutions of SpyCatcher-YlmD used in ciprofloxacin degradation experiment. Initial lane represents Page Ruler. Lanes from 2 to 7 stand for different concentrations of reference protein, i.e. 50 µg/mL, 100 µg/mL, 250 µg/mL, 500 µg/mL. Lanes 8, 9, and 10 are three different dilutions of SpyCatcher-YlmD fusion protein that were used in the degradation experiment, which were calculated to be 75 µg/mL, 135 µg/mL, and 220 µg/mL, respectively. Fusion® software was used for all of the concentration analysis.

3.8. Verification of CsgA-SpyTag + SpyCatcher-GRFT Complex Formation

The verification of complex formation between CsgA-SpyTag and GRFT fused SpyCatcher domain was assessed once the CsgA-SpyTag fiber expression was demonstrated via CR Staining and TEM imaging as explained previously in Section 3.4. The complex formation was conducted as explained in Section 2.11, and investigated through Western Blot using a 15% SDS-PAGE gel. Seeking for changes in molecular weight of SpyCatcher-GRFT fusion protein was the motivation since SpyCatcher-GRFT would increase in molecular weight if it complexes with CsgA-

SpyTag fibers. It can be concluded from the Western Blot data that, CsgA-SpyTag + SpyCatcher-GRFT complex formation is achieved (Figure 20). I have observed the band corresponding to SpyCatcher-GRFT fusion protein around 30 kDa in the 2nd lane. The last lane where CsgA-SpyTag + SpyCatcher-GRFT sample was loaded is comprised of 3 lanes representing CsgA-SpyTag + SpyCatcher-GRFT complex with band at 45 kDa, SpyCatcher-GRFT fusion protein with band at 30 kDa and CsgA-SpyTag with band at 15 kDa molecular weight. Having observed the complex structure itself and 2 components, I concluded that the complex of CsgA and GRFT has occurred through the strong interaction between SpyTag and SpyCatcher.

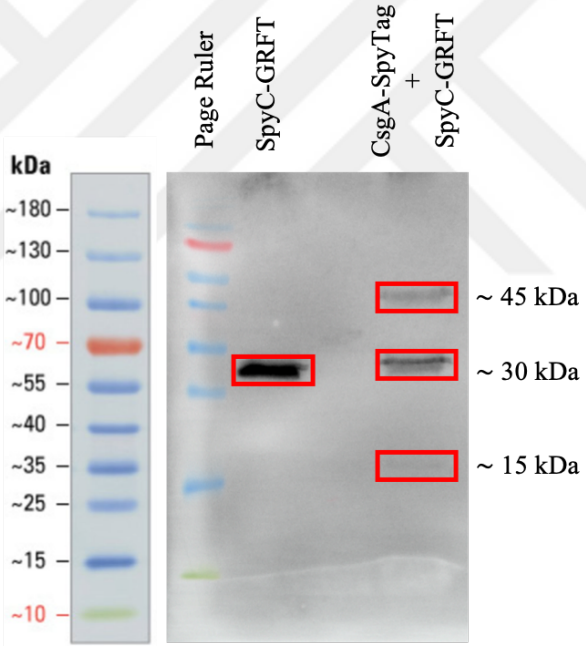

Figure 20. Western Blot for verification of CsgA-SpyTag + SpyCatcher-GRFT complex formation. First lane represents Page Ruler ladder. The 2nd lane stands for SpyCatcher-GRFT fusion protein with a band at 30 kDa. 3rd lane was loaded with CsgA-SpyTag sample however, it could not be observed. The last lane represents CsgA-SpyTag + SpyCatcher-GRFT complex with a band at 45 kDa, SpyCatcher-GRFT fusion protein at 30 kDa, and CsgA-SpyTag with a band at 15 kDa.

3.9. Virus Infectivity Assay After Incubation with CsgA-SpyTag + SpyCatcher-GRFT Complex

The aim of conducting virus infectivity assay with CsgA-SpyTag + SpyCatcher-GRFT complex was to observe if GRFT was able to show its high affinity of binding ability to viral membrane proteins having mannose residues in a complex system of biofilm fibers. The experiment set up was created as explained in Section 2.13. The assay was conducted with 3 different formations of CsgA-SpyTag + SpyCatcher-GRFT complex each with varying concentrations of SpyCatcher-GRFT fusion protein. With this assay, the aim was to observe whether there would be distinctions of SARS-CoV-2 infectivity due to different concentrations of SpyCatcher-GRFT. For higher concentrations of SpyCatcher-GRFT, I expected to see less infectivity for SARS-CoV-2 virus due to antiviral activity of GRFT. Moreover, 30 minutes and 60 minutes of time intervals for incubation of CsgA-SpyTag + SpyCatcher-GRFT complex and SARS-CoV-2 were also assessed in this experiment. The more the incubation period of CsgA-SpyTag + SpyCatcher-GRFT complex and SARS-CoV-2, the less the expected infectivity of SARS-CoV-2. As a control group, CsgA-SpyTag fibers without SpyCatcher-GRFT fusion protein was used. As a result, lower concentration of SpyCatcher-GRFT used in complex formation, i.e. 107 μg/mL, resulted in higher infectivity values of SARS-CoV-2 virus due to having less amount of SpyCatcher-GRFT to interfere with the virus (Figure 21). For complexes having 280 μg/mL and 380 μg/mL of SpyCatcher-GRFT, the infectivity values of SARS-CoV-2 were lower than that of 107 μg/mL for 30 minutes of incubation. Moreover, the infectivity of SARS-CoV-2 after incubation with only CsgA-SpyTag was observed to be higher when compared to complexes with different concentrations of SpyCatcher-GRFT which was expected since there was no GRFT to interfere with

the SARS-CoV-2 virus. In addition, the infectivity of SARS-CoV-2 incubated with only CsgA-SpyTag was a bit lower than the starting titer of SARS-CoV-2 which may be due to the fact that CsgA fibers show some capture of SARS-CoV-2 virus on its own. Overall, for higher concentrations of SpyCatcher-GRFT in the complex and for longer incubation time, the infectivity of SARS-CoV-2 was observed to be reduced. Moreover, considering this specific system related to SARS-CoV-2 capture, it can be concluded that many other enveloped viruses could be captured.

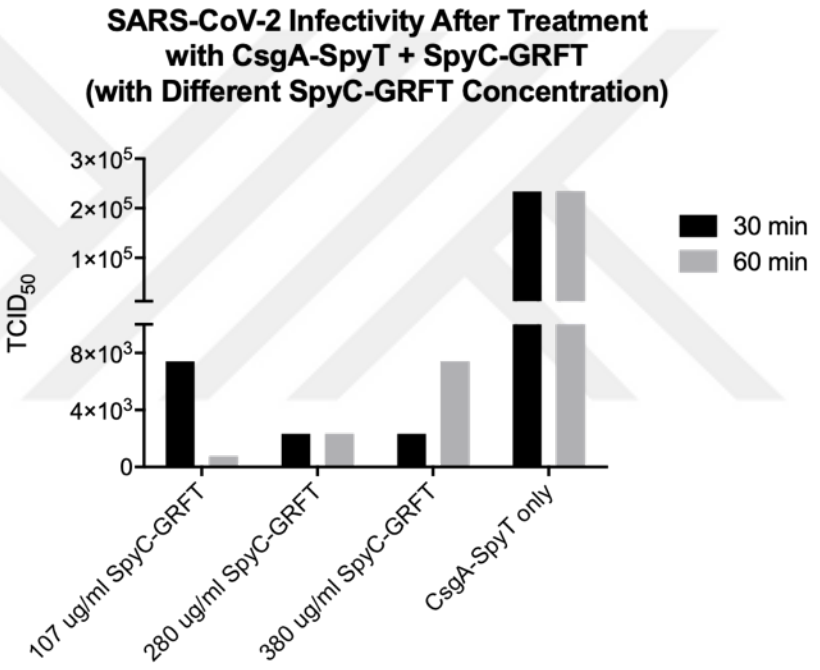

Figure 21. SARS-CoV-2 infectivity analysis after incubation with CsgA-SpyTag + SpyCatcher-GRFT complex with varying concentrations of SpyCatcher-GRFT. For complexes formed with low concentration of SpyCatcher-GRFT, SARS-CoV-2 infectivity latter to incubation was observed to be higher, i.e. CsgA-SpyTag + SpyCatcher-GRFT complex formed with 107 μg/mL SpyCatcher-GRFT. For longer incubation periods, SARS-CoV-2 infectivity after interaction with fiber complex was observed to be lower, i.e. CsgA-SpyTag + SpyCatcher-GRFT complex formed with 107 μg/mL SpyCatcher-GRFT.

3.9.1. Concentration Determination for SpyCatcher-GRFT via Western Blot

Concentrations of SpyCatcher-GRFT used in the complex formation were determined by Western Blot. A calibration curve was formed using a protein of known concentration. The unknown concentrations of studied proteins were analyzed and determined using the standard curve via Fusion® software of Vilber Lourmat imaging system. The reason to quantify the concentration of fusion proteins with Western blotting was the low yield of eluate that was obtained as a result of immobilized metal affinity chromatography (IMAC) purification. Therefore, SpyCatcher-GRFT fusion protein was used without purification but as the soluble part of whole cell lysate and integrated into the experiment with varying volumetric dilutions. Therefore, the concentration measurement of SpyCatcher-GRFT was conducted via Western blot using anti-histag antibodies. Four different concentrations of SpyCatcher-GRFT were used in the experiment, which were determined according to the obtained standard curve (Figure 22). The concentrations were determined to be 280 μg/mL, 380 μg/mL, 380 μg/mL and 107 μg/mL for SpyCatcher-GRFT–1, SpyCatcher-GRFT–2, SpyCatcher-GRFT–3 and SpyCatcher-GRFT–4, respectively. Concentrations of SpyCatcher-GRFT–2 and SpyCatcher-GRFT–3 were calculated to be the same by Fusion® software. Therefore, SpyCatcher-GRFT–2 was excluded from the experiment and continued with 3 different concentrations of SpyCatcher-GRFT.

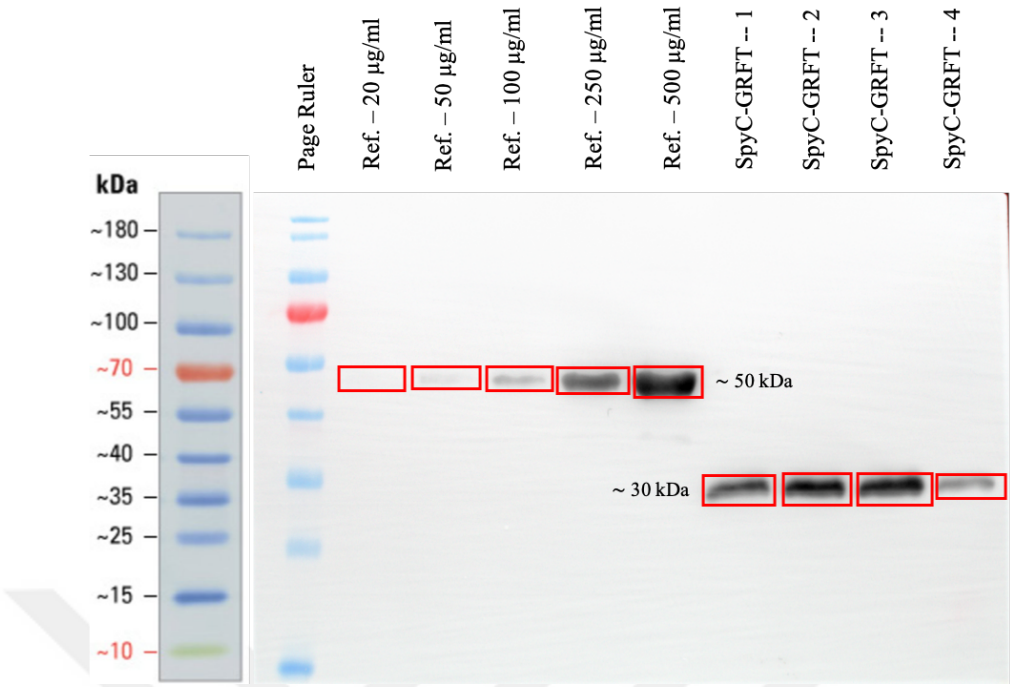

Figure 22. Western blot for concentration determination of different dilutions of SpyCatcher-GRFT used in ciprofloxacin degradation experiment. Initial lane represents Page Ruler. Lanes from 2 to 6 stand for different concentrations of reference protein, i.e. 20 µg/mL, 50 µg/mL, 100 µg/mL, 250 µg/mL, 500 µg/mL. Lanes 7, 8, 9, and 10 are four different dilutions of SpyCatcher-GRFT fusion protein that were used in the degradation experiment, which were calculated to be 280 µg/mL, 380 µg/mL, 380 µg/mL and 107 µg/mL, respectively. Fusion® software was used for all of the concentration analysis.

3.10. Verification of SARS-CoV-2 Virus Capture via TEM & SEM/FIB

The verification of SARS-CoV-2 capture by CsgA-SpyTag + SpyCatcher-GRFT complex was done by imaging the samples using Focused Ion Beam (FIB), which is very similar to Scanning Electron Microscopy (SEM) but with higher resolution, and Transmission Electron Microscopy (TEM). The samples for TEM and FIB imaging were prepared as explained in Section 2.10. TEM images indicated SARS-CoV-2 capture by both CsgA-SpyTag + SpyCatcher-GRFT complex (Figure 23.A, Figure

23.B). I observed spherical particles which have similar dimensions with SARS-CoV-2 virus particles [56] attached to fiber structures of CsgA-SpyTag + SpyCatcher-GRFT. Moreover, CsgA-SpyTag sample was also observed to capture SARS-CoV-2 virus particles (Figure 23.C), however it was not dominant all around the sample where fiber structures were mostly observed (Figure 23.D). This phenomenon was also observed in infectivity assay of SARS-CoV-2 in Section 3.9, where CsgA-SpyTag samples mixed with SARS-CoV-2 also showed capture of virus particles, however it was not as effective as virus capture by CsgA-SpyTag + SpyCatcher-GRFT complex.

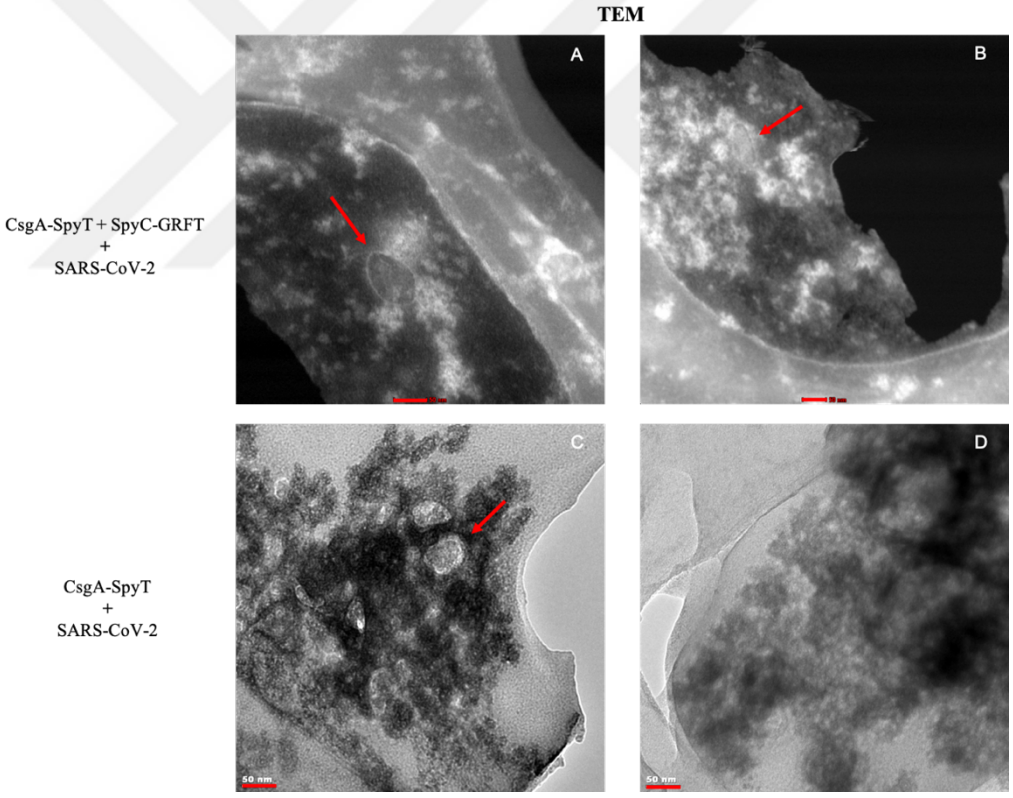

Figure 23. TEM images for SARS-CoV-2 capture by CsgA-SpyTag + SpyCatcher-GRFT complex and CsgA-SpyTag fibers. A. SARS-CoV-2 virus particle captured by mash-like complex structure. B. another SARS-CoV-2 virus particle shown by arrow captured by biofilm fibers functionalized with GRFT. C. SARS-CoV-2 particles

attached to CsgA-SpyTag fibers. D. CsgA-SpyTag biofilm fibers observed in the CsgA-SpyTag incubated with SARS-CoV-2. The red scale bars represent 50 nm.

The same samples of CsgA-SpyTag + SpyCatcher-GRFT complex and CsgA-SpyTag fibers incubated with SARS-CoV-2 were also visualized using FIB. Similar to TEM images, both CsgA-SpyTag + SpyCatcher-GRFT complex and CsgA-SpyTag fibers were observed to capture virus particles (Figure 24). The virus particle clusters observed for CsgA-SpyTag + SpyCatcher-GRFT complex (Figure 24.A) were denser than those observed for CsgA-SpyTag only (Figure 24.C). When compared to TEM, biofilm structures were not as clearly observed in FIB, however fiber-like structures together with attached virus particles were imaged in higher magnification (Figure 24.B and D). The reasons that I could not observe the fiber structures in samples are probably due to dense structure of samples and the coating of Au/Pd prior to imaging, which may be thick for this type of samples.

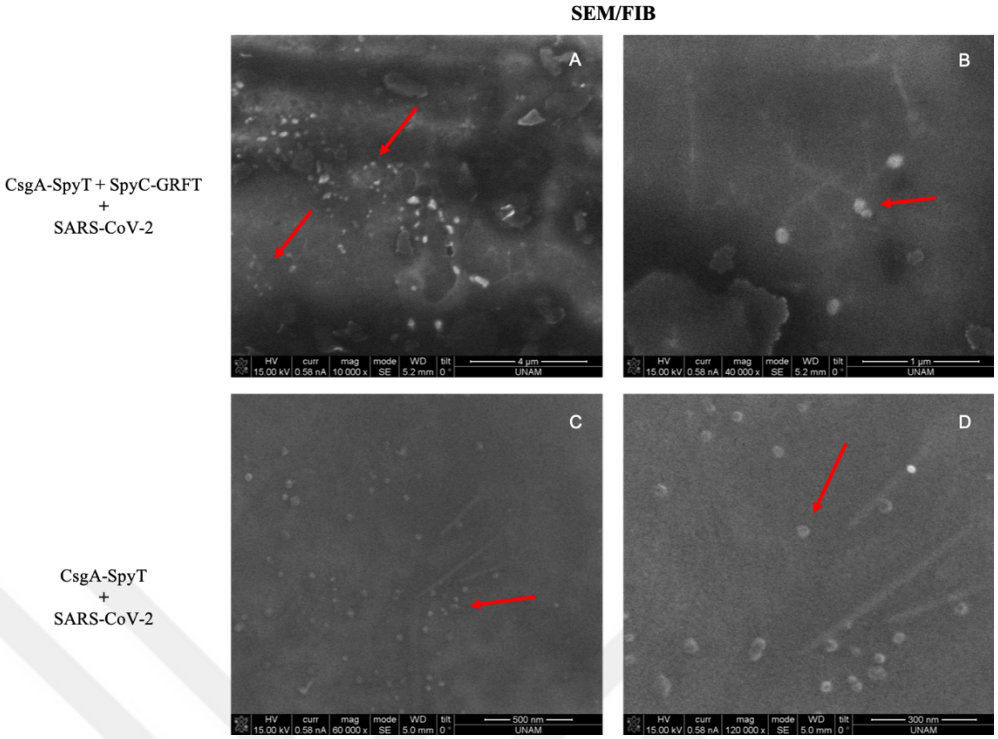

Figure 24. FIB images for SARS-CoV-2 capture by CsgA-SpyTag + SpyCatcher-GRFT complex and CsgA-SpyTag fibers. A. SARS-CoV-2 virus particle captured in clusters by mash-like complex structure observed in the background. B. Captured virus particles with images of CsgA-SpyTag + SpyCatcher-GRFT fibers. C. SARS-CoV-2 particles attached to CsgA-SpyTag fibers. D. CsgA-SpyTag biofilm fibers with SARS-CoV-2 virus particles. The scale bars are 4 µm, 1 µm, 500 nm and 300 nm for A, B, C, D, respectively.

CONCLUSION

Functionalized biofilm proteins are widely used as biomaterials for varying purposes ranging from medicine to environmental applications. Due to their prominent mechanical properties and tendency for genetic modifications, CsgA major curli biofilm protein is considered as a promising component for engineered biomaterial production.

In this study, we aimed to functionalize *E. coli* major curli protein CsgA with two enzymes which are categorized as laccases and with a lectin known for its high binding affinity against viral membrane proteins with mannose groups. Through these functionalization, 3 different biofilm protein complexes were formed via the irreversible, strong isopeptide bond formed between SpyTag and SpyCatcher domains. In this context, 2 of the complexes that were formed initially were CsgA-SpyTag + SpyCatcher-CotA and CsgA-SpyTag + SpyCatcher-YlmD. We checked the complex formation along with enzymatic activity assays for SpyCatcher-CotA and SpyCatcher-YlmD. Once the verifications were done, Ciprofloxacin degradation assays were conducted and as a result antibiotic degradation by both CsgA-SpyTag + SpyCatcher-CotA and CsgA-SpyTag + SpyCatcher-YlmD complexes were achieved. According to the results, it was observed that CotA fused complex structures were better at degradation than YlmD fused complex for the highest concentrations that were used. The last biofilm protein complex structure that we assembled was CsgA-SpyTag + SpyCatcher-GRFT. This complex structure was verified for complex formation between SpyTag fused CsgA and SpyCatcher fused GRFT fusion proteins. Moreover, SARS-CoV-2 infectivity assays were conducted and high binding affinity of GRFT against envelope proteins with multiple mannose groups was also observed in a complex system formed by CsgA fibers.

In this study, we aimed to achieve addition of different functional properties to CsgA biofilm protein, which is a known and well-studied, robust, modifiable protein suitable for many applications regarding biomaterials. We obtained 2 enzyme fused CsgA biofilm complexes and a GRFT fused complex along with the bridging units of SpyTag-SpyCatcher domains. Each one of the complex structures were found to function as they were designed to do so.

As a result, this study showed CsgA biofilm protein could be functionalized with various types of proteins, i.e. enzymes, lectins, via an irreversible bond structured between SpyTag and SpyCatcher domains. The complex structures could be used for coping with pollutants in water bodies such as antibiotics, or they could be functionalized against capturing virus particles from liquid media. In the future, this modular system can be further engineered for integration into physical structures such as filter systems or resins. To sum up, in this study we created a modular platform for functionalizing CsgA biofilm protein with different kinds of functional groups which is open to further modifications according to desired purposes.

BIBLIOGRAPHY

[1] T.R. Jahn, O.S. Makin, K.L. Morris, K.E. Marshall, P. Tian, P. Sikorski, L.C. Serpell, Journal of Molecular Biology 395 (2010) 717–727.

[2] T.P. Knowles, A.W. Fitzpatrick, S. Meehan, H.R. Mott, M. Vendruscolo, C.M. Dobson, M.E. Welland, Science 318 (2007) 1900–1903.

[3] B. Cao, Y. Zhao, Y. Kou, D. Ni, X.C. Zhang, Y. Huang, Proc Natl Acad Sci USA 111 (2014) E5439–E5444.

[4] S. Bhoite, N. van Gerven, M.R. Chapman, H. Remaut, EcoSal Plus 8 (2019) ecosalplus.ESP-0037-2018.

[5] N. Van Gerven, R.D. Klein, S.J. Hultgren, H. Remaut, Trends in Microbiology 23 (2015) 693–706.

[6] A.M. Duraj-Thatte, A. Manjula-Basavanna, J. Rutledge, J. Xia, S. Hassan, A. Sourlis, A.G. Rubio, A. Lesha, M. Zenkl, A. Kan, D.A. Weitz, Y.S. Zhang, N.S. Joshi, Programmable Microbial Ink for 3D Printing of Living Materials Produced from Genetically Engineered Protein Nanofibers, Synthetic Biology, 2021.

[7] A.M. Duraj-Thatte, A. Manjula-Basavanna, N.-M.D. Courchesne, G.I. Cannici, A. Sánchez-Ferrer, B.P. Frank, L. van't Hag, S.K. Cotts, D.H. Fairbrother, R. Mezzenga, N.S. Joshi, Nat Chem Biol (2021).

[8] J. Pu, Y. Liu, J. Zhang, B. An, Y. Li, X. Wang, K. Din, C. Qin, K. Li, M. Cui, S. Liu, Y. Huang, Y. Wang, Y. Lv, J. Huang, Z. Cui, S. Zhao, C. Zhong, Adv. Sci. 7 (2020) 1903558.

[9] R.E. Ahan, B. Saltepe, O. Apaydin, U.O.S. Seker, ChemBioChem (2019) cbic.201800767.

[10] E. Kalyoncu, R.E. Ahan, T.T. Olmez, U.O. Safak Seker, RSC Adv. 7 (2017) 32543–32551.

[11] L. Gianfreda, F. Xu, J.-M. Bollag, Bioremediation Journal 3 (1999) 1–26.

[12] R. Chandra, P. Chowdhary, Environ. Sci.: Processes Impacts 17 (2015) 326–342.

[13] C.F. Thurston, Microbiology 140 (1994) 19–26.

[14] P.S. Chauhan, B. Goradia, A. Saxena, 3 Biotech 7 (2017) 323.

[15] W. Du, C. Sun, J. Liang, Y. Han, J. Yu, Z. Liang, Journal of Food Biochemistry 39 (2015) 101–108.

[16] T.-N. Wang, M. Zhao, Appl Microbiol Biotechnol 101 (2017) 685–696.

[17] Z.-B. Guan, Y. Shui, C.-M. Song, N. Zhang, Y.-J. Cai, X.-R. Liao, Environ Sci Pollut Res 22 (2015) 9515–9523.

[18] T.A.R. Fernandes, W.B. da Silveira, F.M.L. Passos, T.D. Zucchi, AiM 04 (2014) 285–296.

[19] A. Prins, L. Kleinsmidt, N. Khan, B. Kirby, T. Kudanga, J. Vollmer, J. Pleiss, S. Burton, M. Le Roes-Hill, Enzyme and Microbial Technology 68 (2015) 23–32.

[20] F.J. Enguita, P.M. Matias, L.O. Martins, D. Plácido, A.O. Henriques, M.A. Carrondo, Acta Crystallogr D Biol Crystallogr 58 (2002) 1490–1493.

[21] F.J. Enguita, L.O. Martins, A.O. Henriques, M.A. Carrondo, Journal of Biological Chemistry 278 (2003) 19416–19425.

[22] uniprot, (n.d.).

[23] A. Prieto, M. Möder, R. Rodil, L. Adrian, E. Marco-Urrea, Bioresource Technology 102 (2011) 10987–10995.

[24] M. Čvančarová, M. Moeder, A. Filipová, T. Cajthaml, Chemosphere 136 (2015) 311–320.
[25] L. Pan, J. Li, C. Li, X. Tang, G. Yu, Y. Wang, Journal of Hazardous Materials 343 (2018) 59–67.
[26] Lee, Marine Drugs 17 (2019) 567.
[27] S. Lusvarghi, C. Bewley, Viruses 8 (2016) 296.
[28] J.L. Fuqua, V. Wanga, K.E. Palmer, BMC Biotechnol 15 (2015) 12.
[29] P. Emau, B. Tian, B.R. O?keefe, T. Mori, J.B. McMahon, K.E. Palmer, Y. Jiang, G. Bekele, C.C. Tsai, J Med Primatol 36 (2007) 244–253.
[30] T. Mori, B.R. O'Keefe, R.C. Sowder, S. Bringans, R. Gardella, S. Berg, P. Cochran, J.A. Turpin, R.W. Buckheit, J.B. McMahon, M.R. Boyd, Journal of Biological Chemistry 280 (2005) 9345–9353.
[31] P. Meuleman, A. Albecka, S. Belouzard, K. Vercauteren, L. Verhoye, C. Wychowski, G. Leroux-Roels, K.E. Palmer, J. Dubuisson, Antimicrob. Agents Chemother. 55 (2011) 5159–5167.
[32] K.B. Alexandre, E.S. Gray, R. Pantophlet, P.L. Moore, J.B. McMahon, E. Chakauya, B.R. O'Keefe, R. Chikwamba, L. Morris, Journal of Virology 85 (2011) 9039–9050.
[33] B.R. O'Keefe, B. Giomarelli, D.L. Barnard, S.R. Shenoy, P.K.S. Chan, J.B. McMahon, K.E. Palmer, B.W. Barnett, D.K. Meyerholz, C.L. Wohlford-Lenane, P.B. McCray, J Virol 84 (2010) 2511–2521.
[34] J.K. Millet, K. Séron, R.N. Labitt, A. Danneels, K.E. Palmer, G.R. Whittaker, J. Dubuisson, S. Belouzard, Antiviral Research 133 (2016) 1–8.
[35] R.E. Ahan, A. Hanifehnezhad, E. Şahin Kehribar, T.C. Oguzoglu, K. Földes, C.E. Özçelik, N. Filazi, S. Öztop, S. Önder, E.U. Bozkurt, K. Ergünay, A. Özkul, U.Ö. Şafak Şeker, A Highly Potent SARS-CoV-2 Blocking Lectin Protein, Biochemistry, 2021.
[36] B. Zakeri, J.O. Fierer, E. Celik, E.C. Chittock, U. Schwarz-Linek, V.T. Moy, M. Howarth, Proceedings of the National Academy of Sciences 109 (2012) E690–E697.
[37] R.M. Hagan, R. Björnsson, S.A. McMahon, B. Schomburg, V. Braithwaite, M. Bühl, J.H. Naismith, U. Schwarz-Linek, Angew. Chem. Int. Ed. 49 (2010) 8421–8425.
[38] I.N.A. Khairil Anuar, A. Banerjee, A.H. Keeble, A. Carella, G.I. Nikov, M. Howarth, Nat Commun 10 (2019) 1734.
[39] A.H. Keeble, M. Howarth, Chem. Sci. 11 (2020) 7281–7291.
[40] T. Peschke, P. Bitterwolf, S. Gallus, Y. Hu, C. Oelschlaeger, N. Willenbacher, K.S. Rabe, C.M. Niemeyer, Angew. Chem. Int. Ed. 57 (2018) 17028–17032.
[41] J. Bao, N. Liu, L. Zhu, Q. Xu, H. Huang, L. Jiang, J. Agric. Food Chem. 66 (2018) 8061–8068.
[42] G.P. Anderson, J.L. Liu, L.C. Shriver-Lake, D. Zabetakis, V.A. Sugiharto, H.-W. Chen, C.-R. Lee, G.N. Defang, S.-J.L. Wu, N. Venkateswaran, E.R. Goldman, Anal. Chem. 91 (2019) 9424–9429.
[43] Z. Botyanszki, P.K.R. Tay, P.Q. Nguyen, M.G. Nussbaumer, N.S. Joshi, Biotechnol. Bioeng. 112 (2015) 2016–2024.
[44] A.Y. Chen, Z. Deng, A.N. Billings, U.O.S. Seker, M.Y. Lu, R.J. Citorik, B. Zakeri, T.K. Lu, Nature Mater 13 (2014) 515–523.
[45] N.-M. Dorval Courchesne, A. Duraj-Thatte, P.K.R. Tay, P.Q. Nguyen, N.S. Joshi, ACS Biomater. Sci. Eng. 3 (2017) 733–741.

[46] M.L. Evans, E. Gichana, Y. Zhou, M.R. Chapman, in: E.M. Sigurdsson, M. Calero, M. Gasset (Eds.), Amyloid Proteins, Springer New York, New York, NY, 2018, pp. 267–288.
[47] C. Reichhardt, A.N. Jacobson, M.C. Maher, J. Uang, O.A. McCrate, M. Eckart, L. Cegelski, PLoS ONE 10 (2015) e0140388.
[48] J.A. Bornhorst, J.J. Falke, in: Methods in Enzymology, Elsevier, 2000, pp. 245–254.
[49] P.Q. Nguyen, Z. Botyanszki, P.K.R. Tay, N.S. Joshi, Nat Commun 5 (2014) 4945.
[50] S. Rodriguez-Mozaz, I. Vaz-Moreira, S. Varela Della Giustina, M. Llorca, D. Barceló, S. Schubert, T.U. Berendonk, I. Michael-Kordatou, D. Fatta-Kassinos, J.L. Martinez, C. Elpers, I. Henriques, T. Jaeger, T. Schwartz, E. Paulshus, K. O'Sullivan, K.M.M. Pärnänen, M. Virta, T.T. Do, F. Walsh, C.M. Manaia, Environment International 140 (2020) 105733.
[51] L. Lien, N. Hoa, N. Chuc, N. Thoa, H. Phuc, V. Diwan, N. Dat, A. Tamhankar, C. Lundborg, IJERPH 13 (2016) 588.
[52] M. Gros, S. Rodríguez-Mozaz, D. Barceló, Journal of Chromatography A 1292 (2013) 173–188.
[53] S. Aydin, M.E. Aydin, A. Ulvi, H. Kilic, Environ Sci Pollut Res 26 (2019) 544–558.
[54] M.S. Kostich, A.L. Batt, J.M. Lazorchak, Environmental Pollution 184 (2014) 354–359.
[55] N.L. Kennedy Neth, C.M. Carlin, O.S. Keen, Environ. Sci.: Water Res. Technol. 5 (2019) 1222–1233.
[56] Z. Ke, J. Oton, K. Qu, M. Cortese, V. Zila, L. McKeane, T. Nakane, J. Zivanov, C.J. Neufeldt, B. Cerikan, J.M. Lu, J. Peukes, X. Xiong, H.-G. Kräusslich, S.H.W. Scheres, R. Bartenschlager, J.A.G. Briggs, Nature 588 (2020) 498–502.

APPENDIX A

DNA SEQUENCES OF CONSTRUCTS

Table A. 1. DNA Sequences Used in This Study

Gene	Sequence
E. coli csgA gene with native N42 signal sequence	ATGAAACTTTTAAAAGTAGCAGCAATTGCAGCAATCGTA TTCTCCGGTAGCGCTCTGGCAGGTGTTGTTCCTCAGTACG GCGGCGGCGGTAACCACGGTGGTGGCGGTAATAATAGC GGCCCAAATTCTGAGCTGAACATTTACCAGTACGGTGGC GGTAACTCTGCACTTGCTCTGCAAACTGATGCCCGTAAC TCTGACTTGACTATTACCCAGCATGGCGGCGGTAATGGT GCAGATGTTGGTCAGGGCTCAGATGACAGCTCAATCGAT CTGACCCAACGTGGCTTCGGTAACAGCGCTACTCTTGAT CAGTGGAACGGCAAAAATTCTGAAATGACGGTTAAACA GTTCGGTGGTGGCAACGGTGCTGCAGTTGACCAGACTGC ATCTAACTCCTCCGTCAACGTGACTCAGGTTGGCTTTGGT AACAACGCGACCGCTCATCAGTAC
B. subtilis *ylmD* gene	ATGAATACATATCACCCATTCAGTCTTACCACACCCTCG ACACTCATGATACAAGACTGGGCTCAAACGAATCAAAA CAACAAAGAGGTCATTGCCGGATTTACGACAAAAAACG GCGGTGTCAGCCAAAAGCCTTTTGAATCGTTAAATACAG GATTGCACGTTCATGACAAAGATGCAGATGTAGTTAAAA ATCGTGAATATATTGCCGATATGTTTAATACTGATTTGCA GTCTTGGGTATTCGCTGATCAGACACATGATAATCGCGT

	TCAGAAAGTGACGCAGAGGGATAGGGGAAAAGGCGCCC GTGAGTATCACACGGCTCTAAAAGCAACGGACGGGATC TATACAAATGAAAAAAATGTATTTTTAGCATTATGCTTT GCTGATTGTGTGCCTCTTTTCTTTTATGATCCGGTTAAGT CGCTTGTCGGAGTCGCCCATGCCGGGTGGAAAGGCACCG TCAAACAGATTGGCAGAGAAATGGTGAAGCAATGGACT GAGAAGGAAGGTTCAAATCCCTCAGATATTTACGCTGTT ATTGGCCCGTCTATCAGCGGAGCATGCTATACGGTAGAC GACCGCGTCATGGATGCTGTCCGCGCATTGCCGGTTTCA GCAGACCTTGCCGCCAATCAGACGGCAAAGGCACAATA TCAGCTTGATCTGAAAGAGCTGAACCGTCTTATACTGAT GGACAGCGGTTTGGCAAGTGAACAAATTTCTGTCAGCGG TTTATGCACGGAAAGCGAGCCGTCTCTTTTCTATTCTCAT CGCCGCGATCAGGGGAAAACTGGACGGATGATGTCCTTT ATCGGAATGAAGGAGGCA
B. subtilis cotA gene	ATGACACTTGAAAAATTTGTGGATGCTCTCCCAATCCCA GATACACTAAAGCCAGTACAGCAATCAAAAGAAAAAAC ATACTACGAAGTCACCATGGAGGAATGCACTCATCAGCT CCATCGCGATCTCCCTCCAACCCGCCTGTGGGGCTACAA CGGCTTATTTCCGGGACCGACCATTGAGGTTAAAAGAAA TGAAAACGTATATGTAAAATGGATGAATAACCTTCCTTC CACGCATTTCCTTCCGATTGATCACACCATTCATCACAGT GACAGCCAGCATGAAGAGCCCGAGGTAAAGACTGTTGT TCATTTACACGGCGGCGTCACGCCAGATGATAGTGACGG GTATCCGGAGGCTTGGTTTTCCAAAGACTTTGAACAAAC

	AGGACCTTATTTCAAAAGAGAGGTTTATCATTATCCAAA CCAGCAGCGCGGGGCTATATTGTGGTATCACGATCACGC CATGGCGCTCACCAGGCTAAATGTCTATGCCGGACTTGT CGGTGCATATATCATTCATGACCCAAAGGAAAAACGCTT AAAACTGCCTTCAGACGAATACGATGTGCCGCTTCTTAT CACAGACCGCACGATCAATGAGGATGGTTCTTTGTTTTA TCCGAGCGCACCGGAAAACCCTTCTCCGTCACTGCCTAA TCCTTCAATCGTTCCGGCTTTTTGCGGAGAAACCATACTC GTCAACGGGAAGGTATGGCCATACTTGGAAGTCGAGCC AAGGAAATACCGATTCCGTGTCATCAACGCCTCCAATAC AAGAACCTATAACCTGTCACTCGATAATGGCGGAGATTT TATTCAGATTGGTTCAGATGGAGGGCTCCTGCCGCGATC TGTTAAACTGAATTCTTTCAGCCTTGCGCCTGCTGAACGT TACGATATCATCATTGACTTCACAGCATATGAAGGAGAA TCGATCATTTTGGCAAACAGCGCGGGCTGCGGCGGTGAC GTCAATCCTGAAACAGATGCGAATATCATGCAATTCAGA GTCACAAAACCATTGGCACAAAAAGACGAAAGCAGAAA GCCGAAGTACCTCGCCTCATACCCTTCGGTACAGCATGA AAGAATACAAAACATCAGAACGTTAAAACTGGCAGGCA CCCAGGACGAATACGGCAGACCCGTCCTTCTGCTTAATA ACAAACGCTGGCACGATCCCGTCACAGAAACACCAAAA GTCGGCACAACTGAAATATGGTCCATTATCAACCCGACA CGCGGAACACATCCGATCCACCTGCATCTAGTCTCCTTC CGTGTATTAGACCGGCGGCCGTTTGATATCGCCCGTTAT CAAGAAAGCGGGGAATTGTCCTATACCGGTCCGGCTGTC

	CCGCCGCCGCCAAGTGAAAAGGGCTGGAAAGACACCAT TCAAGCGCATGCAGGTGAAGTCCTGAGAATCGCGGCGA CATTCGGTCCGTACAGCGGACGATACGTATGGCATTGCC ATATTCTAGAGCATGAAGACTATGACATGATGAGACCGA TGGATATAACTGATCCCCATAAATAA
Griffithsin gene	ATGGGTAGCAGCCACCATCATCATCACCACAGCAGCGGT CTGGTTCCGCGTGGTAGCCTGACCCATCGCAAATTCGGT GGCAGCGGTGGTAGCCCGTTTAGCGGTCTGAGCAGCATT GCAGTGCGCAGTGGTAGCTACCTGGATGCCATCATCATC GATGGCGTGCATCATGGTGGTAGCGGTGGTAATCTGAGC CCGACCTTTACCTTTGGCAGCGGCGAGTACATTAGCAAC ATGACCATCCGCAGCGGCGACTATATCGACAACATCAGC TTCGAGACCAACATGGGTCGCCGCTTCGGTCCGTATGGT GGTAGTGGTGGTAGCGCCAATACCCTGAGCAACGTGAA GGTGATCCAGATCAACGGTAGCGCAGGCGATTATCTGGA TAGCCTGGATATTTATTATGAACAGTATTAATAA
S. pyogenes SpyCatcher gene with His-Tag	ATGGGTAGCAGCCACCATCATCATCACCACACTAGTGAA AACCTGTATTTTCAGGGCGCCATGGTTGATACCTTATCA GGTTTATCAAGTGAGCAAGGTCAGTCCGGTGATATGACA ATTGAAGAAGATAGTGCTACCCATATTAAATTCTCAAAA CGTGATGAGGACGGCAAAGAGTTAGCTGGTGCAACTAT GGAGTTGCGTGATTCATCTGGTAAAACTATTAGTACATG GATTTCAGATGGACAAGTGAAAGATTTCTACCTGTATCC AGGAAAATATACATTTGTCGAAACCGCAGCACCAGACG GTTATGAGGTAGCAACTGCTATTACCTTTACAGTTAATG

	AGCAAGGTCAGGTTACTGTAAATGGCAAAGCAACTAAA GGTGACGCTCATATT
S. pyogenes SpyTag gene	GCGCATATCGTGATGGTGGATGCGTATAAACCGACCAAA
Double GS Linker	GGTGGCGGTGGTAGCGGTGGCGGTGGTAGC
His-Tag	CACCACCACCACCACCAC

APPENDIX B

LIST OF PRIMERS

Table B. 1. Primer Sequences Used for Cloning of Constructs

Primer Name	**Sequence (5' – 3')**
GO16	GCTACCACCGCCACCGCTACCACCGCCACCGTACTG ATGAGCGGTCG
GO17	GGTGGCGGTGGTAGCGGTGGCGGTGGTAGCATGAAT ACATATCACCCATTCAGTC
GO18	GTGGTGGTGGTGGTGGTGGGATCCTGCCTCCTTCATT CCGATAAAG
GO20	ACCACGCGGAACCAGACCGCTGCTGGATCCAATATG AGCGTCACCTTTAGTTGC
GO21	CACACTAGTGAAAACCTGTATTTTCAGGGCGCCATG GTTGATACCTTATCAGGTTTATCAAG
GO22	GGATCCAGCAGCGGTCTGGTTCCGCGTGGTAGCCTG ACCCATCGCAAATTC
GO23	GGCGCCCTGAAAATACAGGTTTTCACTAGTGTGGTG ATGATGATGGTGGCTGCTA
GO28	TATTGGTGGCGGTGGTAGCGGATCCATGAATACATA TCACCCATTCAGTC
GO29	CTCAGTGGTGGTGGTGGTGGTGCTCGAGTGCCTCCTT CATTCCGATAAAG

GO30	CATGGATCCGCTACCACCGCCACCAATATGAGCGTC ACCTTTAGTTGCTTTGCC
GO31	TATTGGTGGCGGTGGTAGCGGATCCATGACACTTGA AAAATTTGTGGAT
GO32	GTGGTGGTGGTGGTGGTGCTCGAGTTATTTATGGGG ATCAGTTATATCCA
cgA pBD FWD	GGAGAAAGGTACCATGAAACTTTTAAAAGTAGCA
CK42	CTCGAGCACCACCACCACCAC
pbadF1	CTGTTTTGGCGGATGAGAGAA
pbadR1	TTAATTCCTCCTGTTAGCCCAA
pET22B-BB-Rev	GCACCACCACCACCACCAC
pREA11	TCACCTCTTGGATTTGGGTATTAAAGAGGAGAAAGG TACCATGAAACTTTTAAAAGTAGC
pREA30	CATGGTACCTTTCTCCTCTTTAATACCC
pREA145	TGGTGGTGGTGGTGCTCGAGTTATTAATACTGTTCAT AATAAATATCCAGGCTATCCAG
ZK021	GTGGTGGTGGTGGCTACCCTCGAGGTACTGATGAGC GGTCGCG
ZK022	CACCATCACGATATGCGCGGATCCGTGGTGGTGGTG GTGGTGGCTACC
ZK023	GATGCCACGCGTTCATTTGGTCGGTTTATACGCATCC ACCATCACGATATGCGC

APPENDIX C

PLASMID MAPS

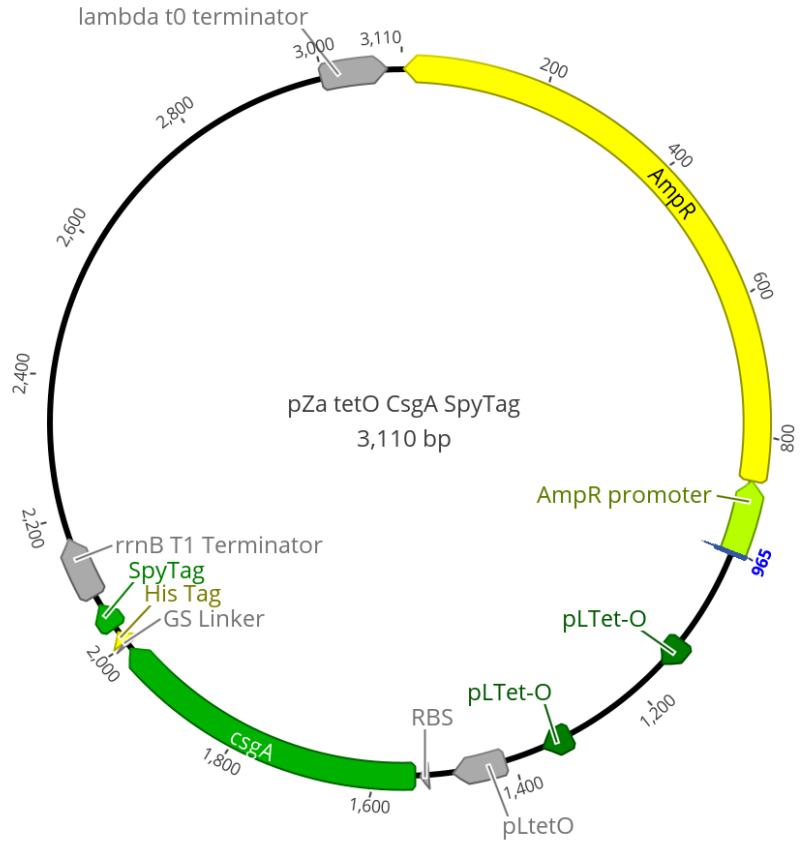

Figure C. 1. Schematic representation of pZa tetO CsgA-SpyTag plasmid

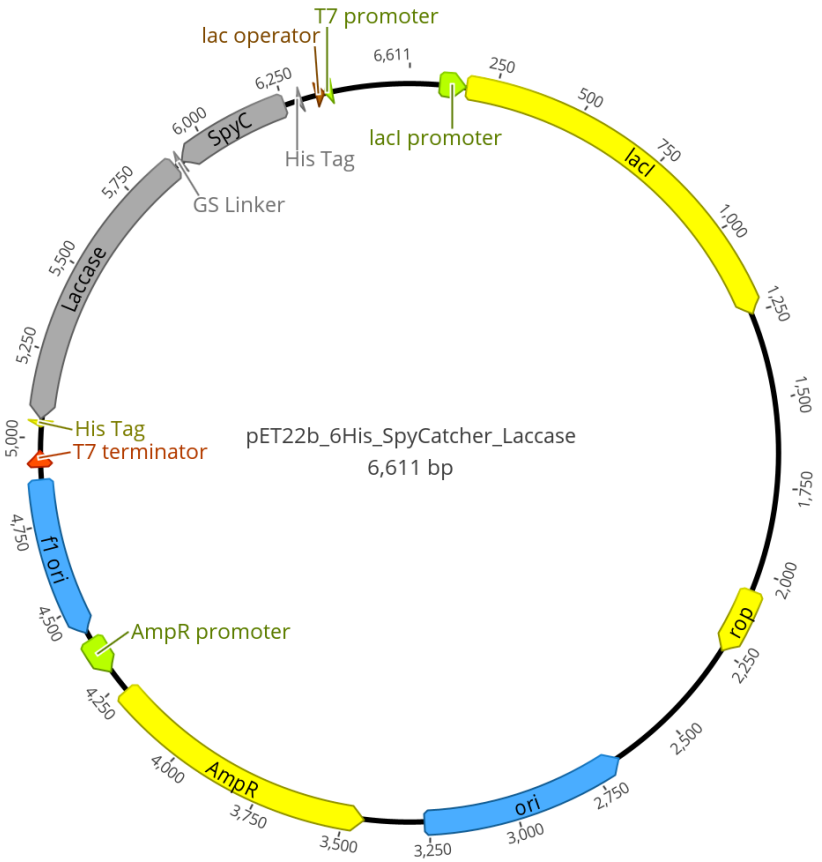

Figure C. 2. Schematic representation of pET22b SpyCatcher YlmD plasmid

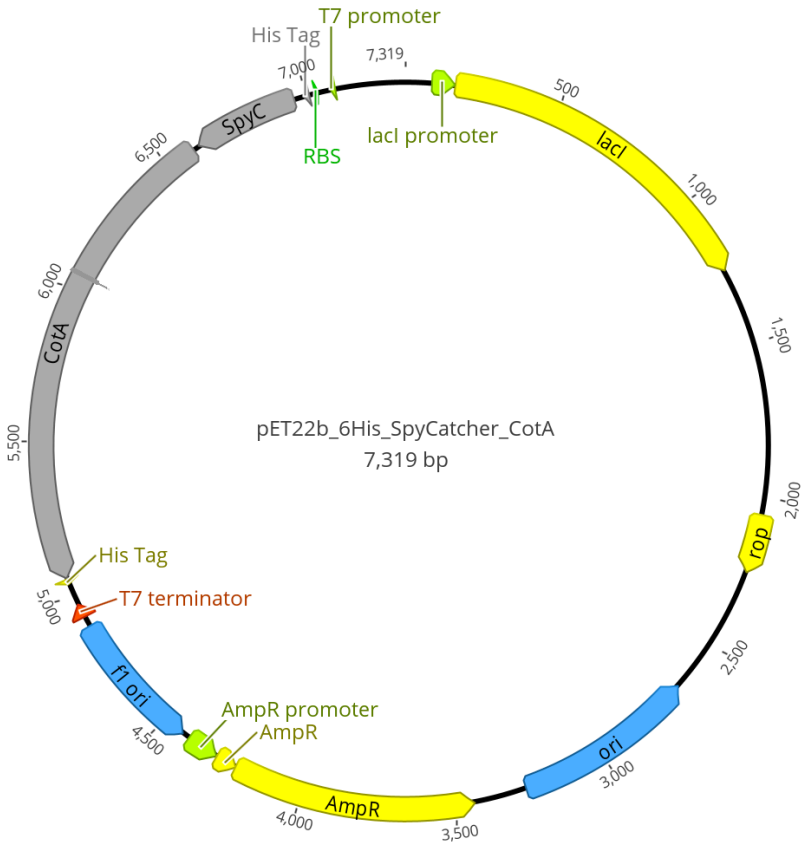

Figure C. 3. Schematic representation of pET22b SpyCatcher CotA plasmid

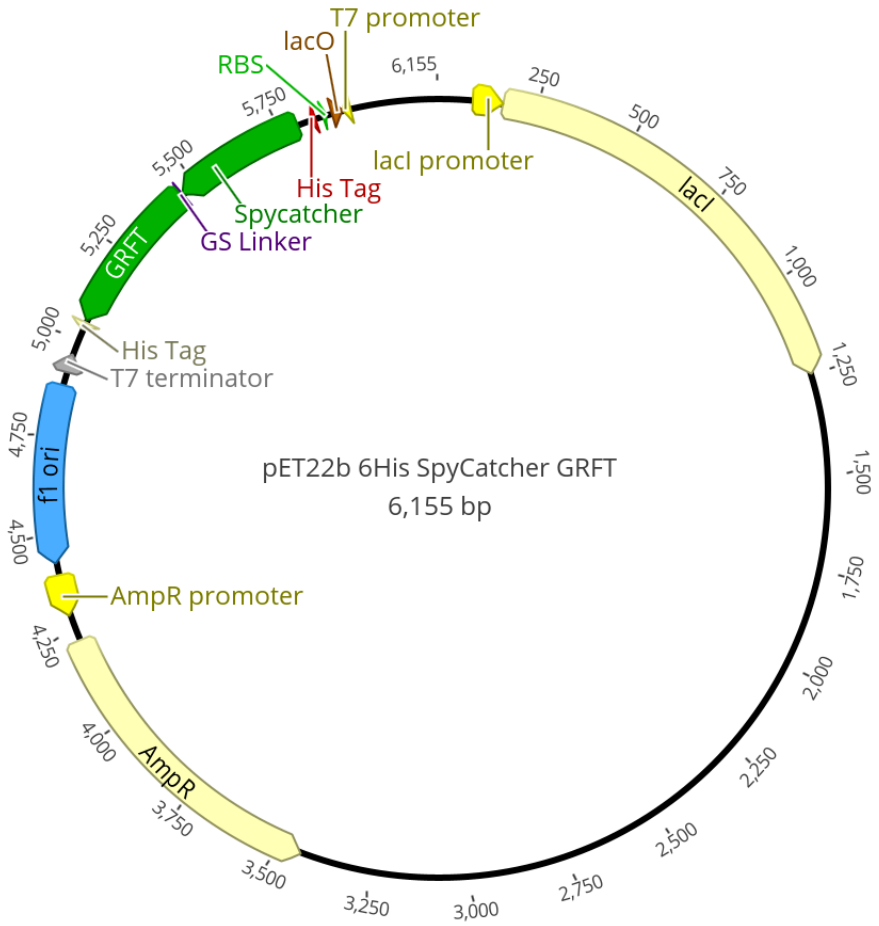

Figure C. 4. Schematic representation of pET22b SpyCatcher GRFT plasmid

APPENDIX D

SEQUENCING RESULTS

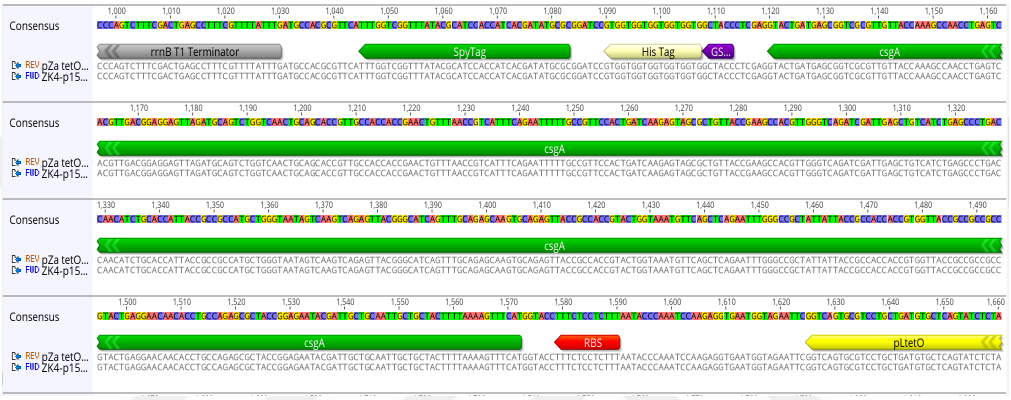

Figure D. 1. Sequence alignment of pZa tetO CsgA SpyTag construct. Alignment performed in Geneious software

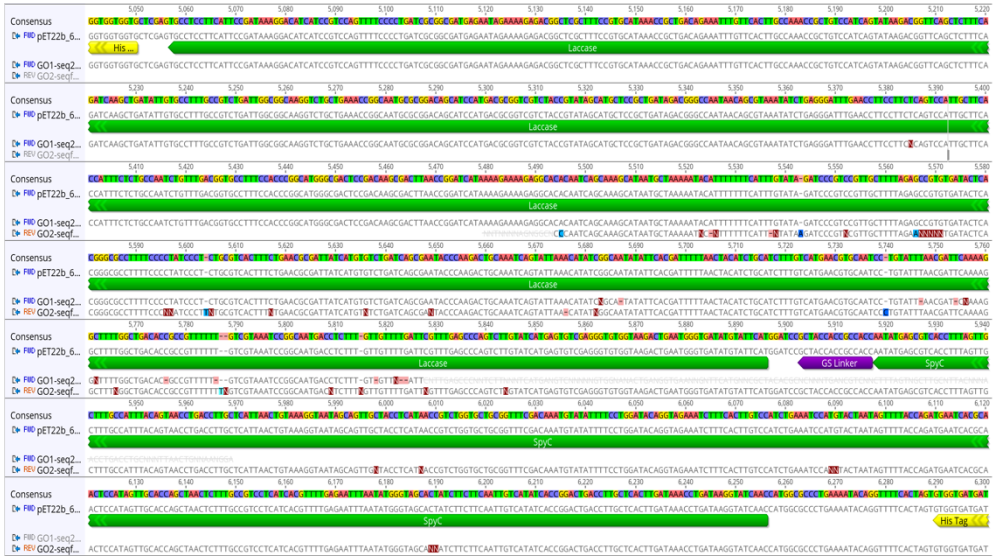

Figure D. 2. Sequence alignment of pET22b SpyCatcher-YlmD construct. Alignment performed in Geneious software

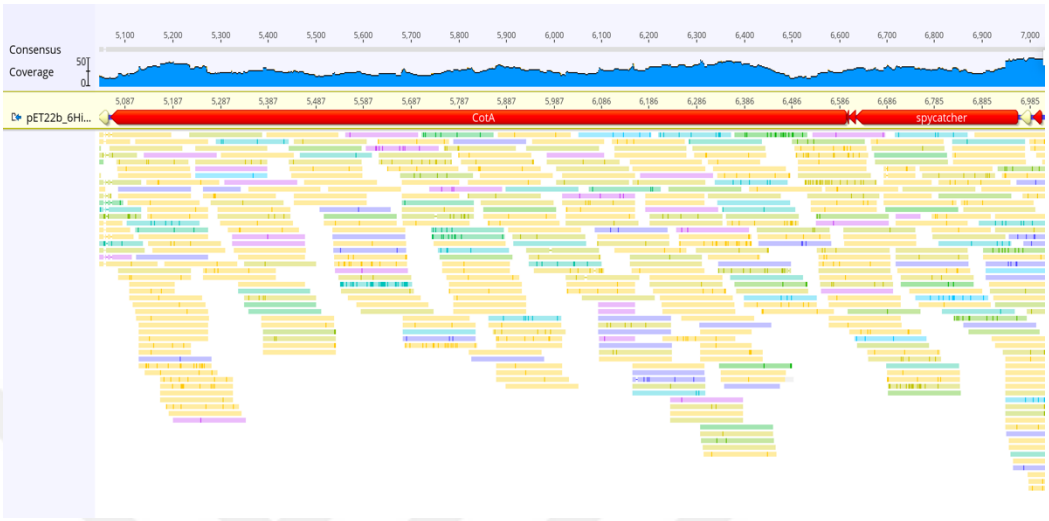

Figure D. 3. Sequence alignment of pET22b SpyCatcher-CotA construct. Alignment performed in Geneious software

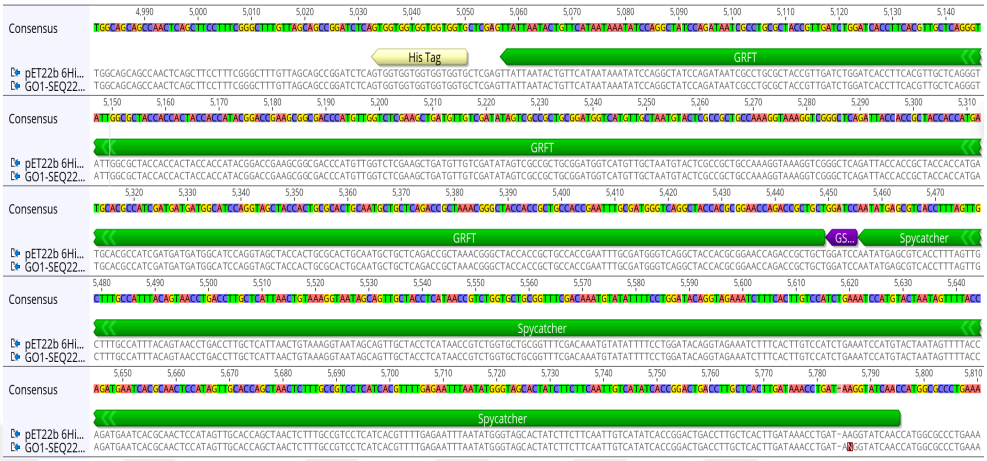

Figure D. 4. Sequence alignment of pET22b SpyCatcher GRFT construct. Alignment performed in Geneious software

APPENDIX E

ADDITIONAL REACTION RECIPES AND CONDITIONS

Table E. 1. Lysogeny Broth (LB) Growth Medium, LB Agar Recipe

Component	**Amount**
Tryptone	10 g
Sodium Chloride (NaCl)	10 g
Yeast Extract	5 g
Agar (only for LB Agar preparation)	15 g
H_2O	1000 ml

Table E. 2. 1X M63 Minimal Medium

Component	**Amount**
$(NH_4)_2SO_4$	2 g
KH_2PO_4	13.6 g
$FeSO_4.7H_2O$	0.5 mg
H_2O	1000 ml

Table E. 3. Double Digestion Reaction Set Up with Restriction Enzymes

10X Cut Smart Buffer	2 µl
DNA	1 µg
Restriction Enzyme 1	0.4 µl
Restriction Enzyme 2	0.4 µl
Nuclease Free Water	Up to 20 µl

Table E. 4. PCR Set up with Q5 DNA Polymerase

Components	**Final Concentration**	**For 25 µL Reaction Volume**
5X Q5 Reaction Buffer	1 X	5 µl
10 mM dNTP	200 µM	0.5 µl
10 µM Forward Primer	0.5 µM	1.25 µl
10 µM Reverse Primer	0.5 µM	1.25 µl
Template DNA	< 1 µg	< 1 µg
Q5 DNA Polymerase	0.02 U/µl	0.5 µl
5X Q5 GC Enhancer (Optional)	1 X	5 µl
Nuclease Free Water	To reaction volume	Up to 25 µl

Table E. 5. PCR Conditions of Q5 DNA Polymerase

Step	**Temperature**	**Time**
Initial Denaturation	98 ºC	30 seconds
Denaturation	98 ºC	5 - 10 seconds
Annealing	50 - 72 ºC	10 - 30 seconds
Extension (25 – 35 cycles)	72 ºC	20 - 30 seconds/kb
Final Extension	72 ºC	2 minutes
Hold	+4 ºC	No time limit

Table E. 6. PCR Set up with Pfu DNA Polymerase

Components	**Final Concentration**	**For 25 µl Reaction Volume**
10X Pfu Reaction Buffer	1 X	2.5 µl
10 mM dNTP	200 µM	0.5 µl
10 µM Forward Primer	0.5 µM	1.25 µl
10 µM Reverse Primer	0.5 µM	1.25 µl
Template DNA	< 1 µg	< 1 µg
Pfu DNA Polymerase	0.02 U/µl	0.5 µl
Nuclease Free Water	To reaction volume	Up to 25 µl

Table E. 7. PCR Conditions of Pfu DNA Polymerase

Step	**Temperature**	**Time**
Initial Denaturation	98 ºC	3 minutes
Denaturation	98 ºC	30 seconds
Annealing	50 - 72 ºC	30 seconds
Extension (25 – 35 cycles)	72 ºC	2 minutes/kb
Final Extension	72 ºC	5 minutes
Hold	+4 ºC	No time limit

Table E. 8. Gibson Assembly Mix Recipe (1.33X)

Component	**Amount**
Taq Ligase (40 U/µl)	50 µl
5X Isothermal Buffer	100 µl
T5 Exonuclease (1 U/µl)	2 µl
Phusion Polymerase (2 U/µl)	6.25 µl
Nuclease Free Water	216.75 µl

Table E. 9. 5x Isothermal Buffer Recipe

Component	**Amount**
PEG-8000	25 %
Tris-HCl	500 mM, pH 7.5
$MgCl_2$	50 mM
DTT	50 mM
NAD	5 mM
dNTPs	1 mM each

Table E. 10. T4 Ligation Reaction Recipe

Component	**Amount**
10X T4 DNA Ligase Buffer	2 µl
Vector DNA	50 ng
Insert DNA	Equal molar to vector DNA
T4 DNA Ligase	1 µl
Nuclease Free Water	Up to 20 µl